# INTERNAL ENERGY AND FRAGMENTATION OF IONS PRODUCED IN ELECTROSPRAY SOURCES

**Valérie Gabelica* and Edwin De Pauw***
*Laboratoire de Spectrométrie de Masse, Université de Liège, Institut de Chimie, Liège, Belgium*

*Received 02 May 2003; received (revised) 18 March 2004; accepted 24 March 2004*

*Published online 12 August 2004 in Wiley InterScience (www.interscience.wiley.com) DOI 10.1002/mas.20027*

*This review addresses the determination of the internal energy of ions produced by electrospray ionization (ESI) sources, and the influence of the internal energy on analyte fragmentation. A control of the analyte internal energy is crucial for several applications of electrospray mass spectrometry, like structural studies, construction of reproducible and exportable spectral libraries, analysis of non-covalent complexes. Sections II and III summarize the Electrospray mechanisms and source design considerations which are relevant to the problem of internal energy, and Section IV gives an overview of the interrelationships between ion internal energy, reaction time scale, and analyte fragmentation. In these three sections we tried to make the most important theoretical elements understandable by all ESI users, and their understanding requires a minimal background in physical chemistry. We then present the different approaches used to experimentally determine the ion internal energy, as well as various attempts in modeling the internal energy uptake in electrospray sources. Finally, a tentative comparison between electrospray and other ionization sources is made. As the reader will see, although many reports appeared on the subject, the knowledge in the field of internal energy of ions produced by soft ionization sources is still scarce, because of the complexity of the system, and this is what makes this area of research so interesting. The last section presents some perspectives for future research.* © 2004 Wiley Periodicals, Inc., Mass Spec Rev 24:566–587, 2005

**Keywords:** *internal energy; electrospray; soft ionization mehods; collision-induced dissociation*

## I. INTRODUCTION

The internal energy of a population of ions has a controlling influence on its reactivity. Molecular ions are produced in the source of the mass spectrometer. The full scan mass spectra contain signals corresponding to the surviving molecular ions and the fragment ions formed in the source. The extent of fragmentation depends on the amount of internal energy received in the source. In electron impact (EI), the content of internal energy is high, leading to electronic and vibrational excitation of the ions. EI spectra exhibit a large fragmentation extent as a consequence of fast unimolecular evolution of the primary ionic species. Moreover, as the kinetic energy of the ionizing electrons is precisely fixed (usually to 70 eV), and as the source is working at low pressure, the internal energy distribution of the ions is quite reproducible, whatever the instrument used. The EI spectra can, therefore, be compiled in databases. The application of EI is, however, restricted to compounds with a sufficient vapor pressure.

Many ionization methods have been developed to allow the production of gas phase ions from fragile compounds. Chronologically field desorption (FD), fast atom bombardment (FAB) and secondary ion mass spectrometry (SIMS), electrospray ionization (ESI) (Yamashita & Fenn, 1984; Whitehouse et al., 1985) and matrix-assisted laser desorption/ionization (MALDI) (Karas et al., 1987; Karas & Hillenkamp, 1988), have been developed to extend the field of application of mass spectrometry to non-volatile and thermolabile compounds. These methods are called ''soft'' because, when proper experimental conditions are used, intact molecular ions can be produced with minimal fragmentation. Alternatively, fragmentation can be induced on purpose by changing the instrumental settings of the source. In electrospray, fragmentation is obtained usually by increasing the acceleration voltages in a medium pressure region after the droplet formation (see Section III). In MALDI, fragmentation (called post-source decay, or PSD) is induced by increasing the laser power or by stronger acceleration of the ions through the plume. As in the case of classical ionization methods (EI, CI), structural information can be inferred from the interpretation of fragmentation patterns obtained for small and medium-size ions. Electrospray is also increasingly used for the study of non-covalent assemblies, and the interaction energetics can also be probed by fragmentation induced in the source.

The energetic characteristics of ion production and activation by ESI are, however, much less well defined as compared to EI. The ions need to cross a high-pressure region, where their internal energy can be modified, before they enter the mass analyzer. As a result, spectra may strongly differ upon experimental conditions (pressure, acceleration voltage, nature of the solution and of the gas phase). Multiply charged ions are commonly produced by ESI. Charge distributions can be shifted, non-covalent complexes can be destroyed, and fragmentation extent can be modified. This makes ESI-MS spectra difficult to compare and to reproduce. Powerful methods such as ESI and MALDI will only show their whole potential once the artifacts arising from the transfer of ions from solid phase or solution to

Contract grant sponsor: FNRS (Fonds National de la Recherche Scientifique, Belgium); Contract grant sponsor: University of Liège; Contract grant sponsor: ARC (Actions de Recherche Concertées/ Communauté Française de Belgique); Contract grant sponsor: Alexander von Humboldt foundation.

**Correspondence to:* Valérie Gabelica, Laboratoire de Spectrométrie de Masse, Université de Liège, Institut de Chimie, Bat. B6c, B-4000 Liège, Belgium. E-mail: v.gabelica@ulg.ac.be

low pressure gas phase of the analyzer will be fully understood. This study reviews the efforts made to understand the activation processes of the ions upon emission and transfer in the electrospray sources.

## II. BRIEF OVERVIEW OF THE ELECTROSPRAY PROCESS

The electrospray process is described in detail in several review studies (Gaskell, 1997; Amad et al., 2000; Cole, 2000; Kebarle, 2000; Kebarle & Peschke, 2000; Cech & Enke, 2001), and only the key features are given here, as a reminder.

### A. Production of Charged Droplets

The solution containing the analyte is introduced in a capillary on which a high electric field is applied. The field causes an electrophoretic separation of the positive and negative charges in the solution. In the positive ion mode (when the capillary is set at positive potential), positive ions move towards the counter-electrode and accumulate at the surface of the liquid at the tip. At a critical field, the meniscus at the tip deforms into what is called the ''Taylor cone,'' which continuously produces droplets enriched in positive ions. Reversing the polarity of the power supply can generate negatively charged droplets instead.

In practice, standard electrospray proceeds at flow rates of 1–100 μL/min. High flow rates are sometimes required when ESI is coupled with HPLC, depending on the column diameter. At such flow rates the production of the droplets has to be assisted by a coaxial sheath gas (heated or not) or by ultrasounds (Ikonomou, Blades, & Kebarle, 1991). These variants of electrospray sometimes bear different names, such as ''ionspray,'' ''thermospray,'' etc. The lower the flow rate, the lesser the need for spray assistance. Nanoelectrospray (Wilm & Mann, 1996; Juraschek, Dülcks, & Karas, 1999) (flow rate of a few nL/min) is the quintessence of electrospray: the electric field is sufficient to maintain the continuous production of charged droplets and no gas assistance is needed. Recently, another variation of electrospray, called ''cold-spray,'' has been developed (Yamaguchi, 2003). In that case, the entire source is cooled down, to allow the detection of fragile non-covalent assemblies. It must be noted that the need for different names sometimes comes more from patent than from physico-chemical reasons. In the present study, the term ''electrospray'' will be used to designate all electrohydrodynamic ionization methods (ionization by the application of a high electric field) on liquids infused through a capillary.

### B. Rayleigh Fission of the Droplets

Solvent evaporation occurs because of collisions with a neutral gas. The radius of the droplet decreases at constant charge until the so-called Rayleigh limit, where the Coulombic repulsion between the charges overcomes the surface tension (Gomez & Tang, 1994; Kebarle, 2000). This leads to the Coulomb fission of the droplet: small offspring droplets are produced that carry approximately 2% of the mass and 15% of the charge of the parent droplet. As evaporation carries on, the daughter droplets undergo fission themselves. This is at the origin of the very rapid reduction in size and charge of the droplets.

### C. Production of Desolvated Ions

Two mechanisms are usually supposed to account for the production of desolvated ions in the gas phase: the ion evaporation mechanism, proposed by Iribarne and Thomson (Iribarne & Thomson, 1976; Thomson & Iribarne, 1979; Iribarne, Dziedzic, & Thomson, 1983) and the charged residue mechanism proposed by Dole (Dole, Mack, & Hines, 1968). Historically, these models had been proposed before the droplet fission scheme presented in the above section was established. With the current level of understanding, the two models can be restated as follows (Kebarle, 2000):

- Ion evaporation mechanism (IEM): at an intermediate stage in the droplet's lifetime (critical radius larger than the Rayleigh limit), the electric field on the surface of the droplet is sufficiently high so that solvated ions are emitted (evaporated) directly from the charged droplets.
- Charged residue mechanism (CRM): the charged residue model assumes that the series of droplet fission events leads to a final droplet containing a single analyte molecule (Schmelzeisen-Redeker, Bütfering, & Röllgen, 1989). The last solvent molecules evaporate until the ion is completely desolvated.

Currently it is generally admitted that small ions (salts, . . .) are produced predominantly by the ion evaporation mechanism (Kebarle & Tang, 1993; Wang & Cole, 2000; Gamero-Castaño & Fernandez de la Mora, 2000a), whereas large globular proteins are produced via the charged residue mechanism (Cole, 2000; Gamero-Castaño & Fernandez de la Mora, 2000b). However, Iavarone & Williams (2003), based on the solvent-dependent extent of charging, have provided evidence that even small ions were produced by the charged residue mechanism. This lively debate is, therefore, far from over.

## III. ELECTROSPRAY SOURCE DESIGN

Electrospray is an atmospheric pressure source, but the mass spectrometer must be operated at low pressures ($10^{-3}$ to $10^{-10}$ Torr, depending on the analyzer). The pressure is usually reduced in multiple stages (differential pumping), the different vacuum chambers being separated by small orifices, cones, or capillaries (Fig. 1a–e). Two processes have a great influence on the ion internal energy at this stage. First, supersonic expansion, which is inherent to differential pumping stages separated by small orifices, increases the axial component of the ion velocity and decreases the internal energy (Hayes & Small, 1983). Second, voltage differences in the intermediate pressure region are responsible for acceleration of the ions and/or of the charged droplets. Subsequent collisions with neutral gas causes droplet evaporation, but also ion activation (increase of internal energy). The electrospray source design is, therefore, crucial for internal energy build-up.

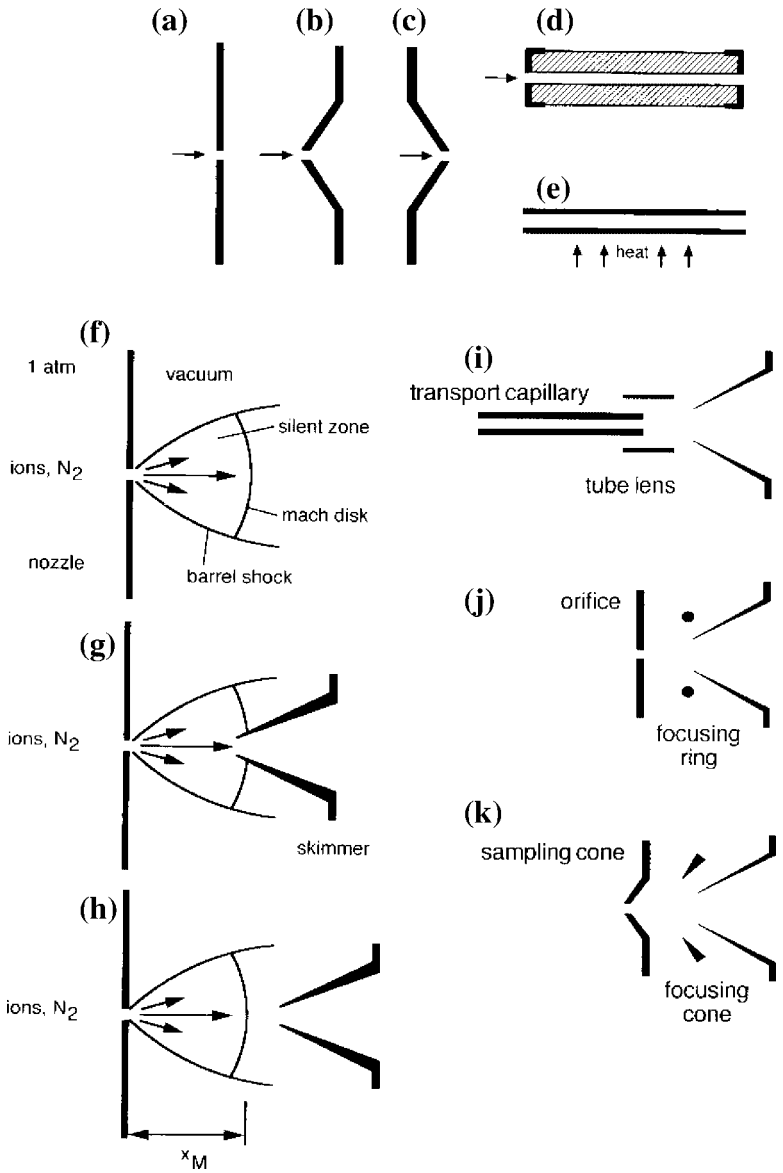


**FIGURE 1.** Different source configurations. (**a–e**): Sampling of ions and gas via different shapes of orifices and tubes; (a) orifice in a flat disk (SCIEX API 100/300); (b) orifice in the top of a cone (Micromass, SCIEX API 3); (c) orifice in the bottom of a cone (Vestec); (d) glass tube with metallized ends (Analytica for HP, Jeol, Bruker, . . .); (e) heated metal tube (ThermoFinnigan). (**f–h**): Free jet expansion of gas and ions into vacuum; (f) basic principle; (g) arrangement with skimmer penetrating into the silent zone; (h) skimmer located more distant than the Mach disk. (**i–k**): Additional focusing items located in the molecular beam stage for forcing ions through the skimmer orifice; (i) tube lens (ThermoFinnigan); (j) ring (SCIEX); (k) cone (Micromass). (Adapted from Bruins AP., ESI source design and dynamic range considerations. In: Electrosrpay Ionization Mass Spectrometry, Cole RB, Editor. Chapter 3, pp 107–136, copyright © 1997 John Wiley and Sons. This material is used by permission of John Wiley and Sons.)

## A. Supersonic Expansion

Only a qualitative description of supersonic expansion is intended here [for more information, see Bruins (1997)]. When a gas flows from a reservoir at pressure $P_0$ into a low-pressure region at pressure $P_1$ through a small orifice of diameter $D_o$, and if $D_o$ is larger than the mean free path in the reservoir, then the collisions in the orifice give the gas a supersonic axial velocity. Molecules in this "silent zone" are shielded from the external medium by a shock wave (barrel shock laterally, and Mach disk in front) (Fig. 1f). The distance from the orifice to the Mach disk ($X_M$) is given by:

$$X_M = 0.67 D_o (P_0/P_1)^{1/2} \quad (1)$$

$X_M$ can range from a few millimeters to several centimeters in heated capillary sources. In supersonic expansion, the axial velocity is increased at the expenses of the radial velocities. At the level of the shock waves (transition between the silent zone and the exterior), the velocities are re-randomized by collisions.

### B. Skimmer Systems

Different kind of sampling items can be used (Bruins, 1997): the orifice can be placed in a flat disk, at the top, or at the bottom of a cone (Fig. 1a–e). Skimmers (cone-shaped metal pieces) are used to sample ions that exit the orifice as a supersonic jet (Pertel, 1975; Campargue, 1984). The electric field caused by the voltage difference between the orifice and the skimmer accelerates the ions through the gas. Collisions of the analyte with the gas increase the ion internal energy. Both the sampling efficiency and the nature of the sampled ions depends on the position of the skimmer relative to the Mach disk. If it penetrates in the silent zone (Fig. 1g), the sampling efficiency is greater than if located beyond the Mach disk (Fig. 1h), because of the large axial component of the velocity in the silent zone. However, ions are colder in the silent zone, and non-fully desolvated droplets, or clusters formed by condensation upon supersonic expansion are more likely to be sampled, which is detrimental to the analytical performances. Beyond the Mach disk, ion trajectories are re-randomized by collisions with the surrounding gas, and ions are warmed up. Ion sampling by skimmers located beyond the Mach disk (Fig. 1h) is, therefore, less efficient, but desolvation and declustering is more effective. In most commercial instruments, additional focusing items (tube lens, focusing ring, or focusing cone) are placed between the orifice and the skimmer, to redirect the ions towards the skimmer and increase sensitivity (Fig. 1i–k). These focusing items also accelerate the ions and, therefore, modulate collisional activation.

### C. Heated Capillary Configuration

In 1990, Chait et al. (Chowdhury, Katta, & Chait, 1990) developed another alternative: ions are transferred from atmospheric pressures to vacuum through a heated stainless steel capillary (Fig. 1e). The temperature of the heated capillary is one more degree of freedom to modulate the internal energy of ions (Rockwood et al., 1991; Busman, Rockwood, & Smith, 1992; Meot-Ner (Mautner) et al., 1995; Penn et al., 1997b; He et al., 1999; Garcia et al., 2001). Some authors (Rockwood et al., 1991; Busman, Rockwood, & Smith, 1992; He et al., 1999) tried to infer Arrhenius parameters from the temperature dependence of the fragmentation extent. However, arguments will be presented in this study which show that this kind of data treatment is not meaningful for quantitative thermochemical studies.

## IV. INFLUENCE OF INTERNAL ENERGY ON THE APPEARANCE OF THE MASS SPECTRA: THEORY

Theoretical considerations which are important for the understanding of the discussions in the following sections are summarized below. For a more detailed discussion, the reader is encouraged to refer to the tutorial article of Vékey (1996). The discussion below is based on an electrospray-single stage mass analyzer (ESI-MS) configuration, and for a single analyte ion fragmenting via two competing channels. The appearance of the mass spectrum depends on different parameters.

### A. Characteristics of the Dissociation Channels

The dissociation rate constant $k$ of an ion depends on its internal energy $E$ (Fig. 2a). The internal energy of an ion is its total energy above its electronic, vibrational, and rotational ground state. The dependency of $k$ versus $E$ can be described by the RRK or the RRKM theories of unimolecular dissociations (Forst, 1973; Gilbert & Smith, 1990; Baer & Mayer, 1997; Steinfeld, Francisco, & Hase, 1999). Starting at the critical energy $E_0$, the dissociation rate increases with internal energy, and different dissociation pathways are characterized by different $k(E)$ curves. The shape of $k(E)$ depends on the potential energy surface along the reaction coordinate. Usually, a cleavage reaction displays a

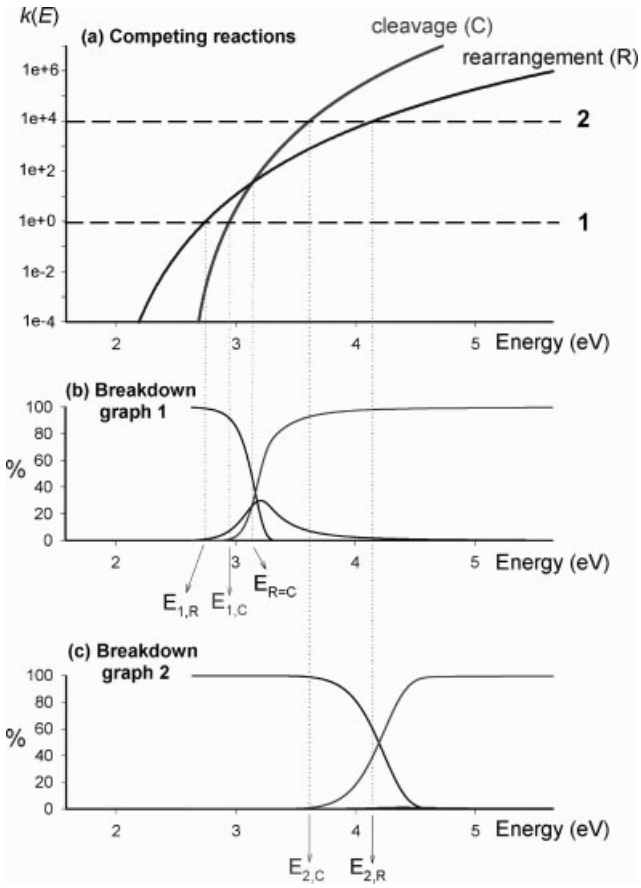


**FIGURE 2.** (**a**) Rate constants as a function of the internal energy for two hypothetical competing reaction channels (a rearrangement and a cleavage reaction). The curves have a RRKM-like dependency, but have been calculated with hypothetical critical energies and frequency sets. The breakdown diagrams for (**b**) instrument 1 ($\tau = 10$ ms) and (**c**) instrument 2 ($\tau = 1$ μs) have been generated with Eqs. 3–6, using the hypothetical $k(E)$ curves displayed in panel (a).

steeper rise in $k(E)$ than a rearrangement reaction. For a molecule which shows both kind of fragmentation, it happens very often that these curves cross at some point. Two such curves are shown in Figure 2a.

### B. Time Scale of the Experiment

The fragmentation extent depends on the dissociation rate, and on the time after which the system is sampled (Pertel, 1975; Vékey, 1996). The ratio between the intensity of the parent ion after a time $\tau$ ($I_M$) and the intensity of the parent ion at $\tau = 0$ ($I_{M,0}$) often assumed to be equal to $I_M + \Sigma I_{fragments} = I_{tot}$ is given by:

$$I_M/I_{M,0} = \exp(-k(E).\tau) \quad (2)$$

The ratio $I_M/I_{M,0}$ is often called the ''survival yield'' of the parent ion. $k(E)$ is the dissociation rate constant which depends on the internal energy as shown above, and $\tau$ is the time scale of the experiment (the time after which the system is sampled, equal to the time allowed to fragment). In some cases $\tau$ can be chosen by the experimentalist (like for example in quadrupole ion trap or in FTICR MS/MS experiments), but in the case of ion dissociation in the electrospray source, $\tau$ is equal to the flight time of the ions between the source and the entrance of the mass analyzer, and, therefore, depends on the hardware configuration of the instrument and on the voltages applied.

The shorter the time scale $\tau$, the larger the dissociation rate must be for a fragment to be observed, and the higher the internal energy must be in order to reach that minimum rate. Let us assume for example that a fragment is detected if its intensity is $\geq$1% of that of the parent ion (i.e., if $I_M/I_{M,0} \leq 0.99$). Therefore, the rate constant $k$ must be $\geq 0.01/\tau$. If $\tau = 10$ ms, then the threshold $k_1$ is 1 $s^{-1}$, and if $\tau = 1$ µs, then the threshold $k_2$ is $10^4$ $s^{-1}$. These two thresholds are represented by horizontal lines in Figure 2a, corresponding to two hypothetical instruments (instrument 2 having a shorter time window than instrument 1). The minimum internal energy necessary for a fragment to be observed is called the apparent threshold for fragmentation. The energy difference between the true threshold and the apparent threshold is called the ''kinetic shift'' (Lifshitz, 1982).

### C. Ion Intensities as a Function of the Internal Energy: The Breakdown Graph

A breakdown graph is a plot of the relative intensities of the parent and the fragment ions as a function of the internal energy of the parent ion. Here, all ions are assumed to have the same internal energy $E$. The relative intensities of the parent ion M, the rearrangement fragment R, and the cleavage fragment C are given by:

$$I_M/I_{tot} = e^{-\Sigma k.\tau} \quad (3)$$

$$I_R/I_{tot} = (k_R(E)/\Sigma k)\left(1-e^{-\Sigma k.\tau}\right) \quad (4)$$

$$I_C/I_{tot} = (k_C(E)/\Sigma k)\left(1 - e^{-\Sigma k.\tau}\right) \quad (5)$$

$$\Sigma k = k_R(E) + k_C(E) \quad (6)$$

The breakdown graph calculated for instrument 1 ($\tau = 10$ ms) using the $k(E)$ curves of Figure 2a is displayed in Figure 2b. A given fragment is observed if its rate constant is larger than the threshold $k_1$ (horizontal line 1). If the internal energy $E$ is lower than $E_{1,R}$, no fragment is observed. If $E_{1,R} < E < E_{1,C}$, only a rearrangement product can be observed, as curve C is still below line 1. The cleavage product starts to appear at $E \geq E_{1,C}$. The rearrangement product R is the most abundant until the energy $E_{R=C}$ (at which the two $k(E)$ curves cross) is reached. At energies $E > E_{R=C}$, the cleavage reaction is faster than the rearrangement, and product C becomes predominant. If instrument 2 ($\tau = 1$ µs) is used instead of instrument 1, higher ion internal energies are needed for the fragments to be observed (Fig. 2c), and cleavage products are now favored at all energies, as the apparent threshold $E_{2,C}$ is smaller than $E_{2,R}$.

We, therefore, see than the breakdown graph depends on the time scale of fragmentation (and, therefore, on the instrument chosen). The range of internal energies of analytical significance (to have a measurable fragmentation extent, i.e., between 1 and 99%) is closely linked to the instrument time scale. For a given time scale, the breakdown diagram, when expressed as a function of the internal energy $E$, is unique for each molecule.

### D. Internal Energy Distributions $P(E)$

#### 1. Definition

When considering a ensemble of molecules, in most cases they do not all have the same internal energy $E$. The internal energy distribution $P(E)$ is a function which describes the probability of a molecule having a particular energy $E$. The distribution $P(E)$ is normalized to unity.

#### 2. Influence on the Breakdown Graphs

The ion ratios defined by the breakdown graph should, therefore, be weighted by the probability of the ion having that particular energy. A distribution $P(E)$ is modulated by all energy input (collisional activation, photon absorption) or energy output (collisional cooling, photon emission) events. Moreover, the dissociation of ions depletes the ion population at energies higher than the critical energy $E_0$. The distribution $P(E)$ is, therefore, changing in time, which in turn influences the observed dissociation rate. Detailed modeling of the activation/deactivation and dissociation processes by master equation modeling are, therefore, required (Dunbar & Zaniewski, 1992; Price & Williams, 1997; Drahos & Vékey, 2001; Dunbar, 2004). Two interesting limiting cases are described below, where the breakdown curves can still be predicted by simple models, but it must be kept in mind that reality is more complicated.

#### 3. Limiting Case 1: Rapid Energy Exchange Compared to Dissociation

In that case, $P(E)$ is determined by the equilibrium established by activation and deactivation events, but is not perturbed by the negligible contribution of the dissociation (Vékey, 1996; Price & Williams, 1997; Dunbar & McMahon, 1998). Moreover, the

internal energy distribution $P(E)$ takes the form of a Boltzmann distribution, and can be characterized by a temperature. The observed dissociation rate constant $k_{obs}$ is the average of the unimolecular rate constant $k(E)$ over the energy distribution $P(E)$:

$$k_{obs} = \int_0^\infty P(E)k(E)\mathrm{d}E \quad (7)$$

In practice, the temperature dependence of the rate constant can be fitted with the Arrhenius equation $k = A \cdot \exp(-E_a/k_B T)$. It can be demonstrated that, in the rapid energy exchange limit, $E_a^{obs}$ is equal to the dissociation enthalpy $+k_B T$ if the reaction has no reverse energy barrier (Laskin & Futrell, 2003; Dunbar, 2004). This is extremely useful for thermochemical studies. This limiting case is applicable only in cases where there is continuous activation and deactivation during the time allowed for fragmentation.

#### *4. Limiting Case 2: No More Energy Exchange During Fragmentation*

This limiting case is particularly useful for describing the fragmentation in ESI-MS. It is assumed that the internal energy distribution is built up in the high-pressure region of the source. No fragmentation is supposed to occur yet at this stage. Once the ions pass the skimmer and travel in the low-pressure region, the ion internal energy distribution is assumed not to change anymore. The time allowed for the ions to fragment is the time elapsed during the trajectory from the skimmer to the entrance of the analyzer.

The ion abundances are, therefore, weighted by the probability $P(E)$ of the ions having a particular internal energy $E$. The total abundance of ion formed or destroyed is calculated by an integral over all possible energies. For a molecule M which gives a single fragment F with a single rate constant $k(E)$ (for sake of simplicity), the ion intensities are given by:

$$I_M/I_{tot} = \int_0^\infty P(E)\mathrm{e}^{-k(E).\tau}\mathrm{d}E \quad (8)$$

$$I_F/I_{tot} = \int_0^\infty P(E)(1 - \mathrm{e}^{-k(E).\tau})\mathrm{d}E \quad (9)$$

## V. ANALYTICAL ASPECTS OF ELECTROSPRAY SOURCE-CID, AND THE UNDERLYING ROLE OF INTERNAL ENERGY

### A. Structure Determination by Source-CID

#### *1. An Alternative to MS/MS*

Collision-induced dissociation spectra are usually obtained by MS/MS: the parent ion is selected, collided with a neutral gas, and the fragment ion spectrum is recorded. However, it has been recognized very early that collisional dissociation could be induced in the electrospray source by increasing the different acceleration voltages (Loo, Udseth, & Smith, 1988; Smith & Barinaga, 1990). Different names for this process have been given by users and manufacturers: nozzle-skimmer fragmentation, cone-voltage fragmentation, skimmer-CID,... In the present study, this will be referred to as "source-CID." The disadvantage is that the parent ion is not selected. Rather, all ions emitted by the electrospray source undergo collisional activation, and all the fragments are collected in the same mass spectrum. Nevertheless, ion selection is not always required, for example in the analysis of pure, or HPLC-separated analytes. Chowdhury, Katta, & Chait (1990) successfully demonstrated this approach for peptide sequencing. Source-CID avoids any requirement for real-time data-dependent scanning softwares, as required for automated MS/MS. A simple ramp of voltages can be applied between the different skimmers and lenses to produce various amounts of fragments during analyte elution.

Structure determination is made by the analysis of the nature and the abundance of the fragments issued from CID. Interestingly, electrospray source-CID sometimes gives different fragments than other CID methods. To illustrate this point, we show here an example of isomer differentiation by electrospray. Laprévote et al. (1996) reported high-energy (keV) CID, LSIMS, and electrospray source-CID of indoloquinolizidine stereoisomers (Fig. 3). The high-energy collision MS/MS spectra obtained on a sector instrument are highly reproducible, and give a fingerprint of the compound structure because of extensive fragmentation of the backbone, but are insensitive to the stereochemistry of the compound (Fig. 3b). LSIMS spectra also show extensive fragmentation (Fig. 3c). In contrast, in electrospray source-CID (Fig. 3d), the *trans*-isomer readily looses ammonia to give the fragment at *m/z* 225, whereas the *cis*-isomer is protected by intramolecular hydrogen bonding. Electrospray source-CID, therefore, favors different fragmentation pathways than high-energy (keV) MS/MS, of LSIMS mass spectra, which allow stereochemical differentiation.

This can be understood in the framework of typical breakdown graphs shown in Figure 2b,c. In high-energy CID MS/MS, cleavage products are favored. The situation is closer to Figure 2c. However, in electrospray source-CID, the time scale and the internal energy scale are different, and closer to the case of Figure 2b. The rearrangement reaction, which is sensitive to ion stereochemistry, can now be favored if very gentle activation conditions are used. Electrospray source-CID, therefore, proceeds on a longer time scale and at lower mean internal energies than MS/MS collision-induced dissociation in the keV range. Several authors have indeed shown that the breakdown curves obtained in source-CID are quite similar to those obtained in MS/MS in quadrupole collision cells (laboratory kinetic energy range: 10–100 eV) (van Dongen et al., 1999; Harrison, 1999a,b).

#### *2. In-Source CID for Mass Spectral Library Searching*

To perform compound identification by library searching, the experimental and the library spectra must be as similar as possible. It is, therefore, crucial that equivalent source conditions

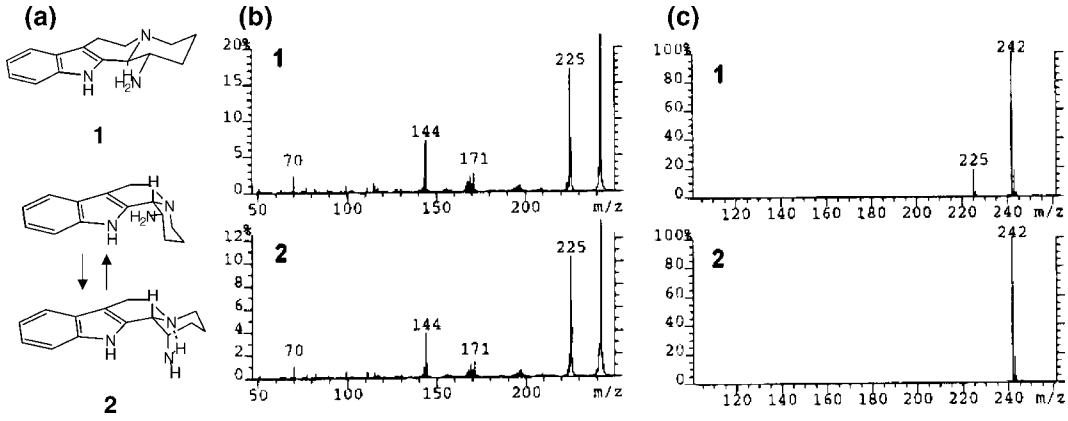


**FIGURE 3.** (**a**) Structure of the indoloquinolizidine stereoisomers **1** and **2** (m = 242 Da). (**b**) Collision-induced dissociation spectra of $\mathbf{1}H^+$ (**top**) and $\mathbf{2}H^+$ (**bottom**) at 4 keV collision energy. (**c**) Electrospray mass spectra of $\mathbf{1}H^+$ (**top**) and $\mathbf{2}H^+$ (**bottom**) recorded with a difference of 24 V between the sampling cone and the skimmer voltages. (Laprévote O, Ducrot P, Thal C, Serani L, Das BC. Stereochemistry of electrosprayed ions. Indoloquinolizidine derivatives. J Mass Spectrom 31:1149–1155, Copyright © 1996 John Wiley and Sons. This material is used by permission of John Wiley and Sons.)

are used for constructing the library and for recording the experimental spectra. More importantly, the libraries should be exportable, i.e., they should be valid for any instrument. This is more difficult to achieve, for different instruments have different source configurations (see Section III), and, therefore, a given voltage on one source is not equivalent to the same voltage on another source in terms of resulting ion activation. Moreover, an inter-laboratory comparison has shown that significantly different spectra can be obtained on several instruments of the same type (Bogusz et al., 1999). A calibration of the source conditions may, therefore, be required for each instrument (not only each instrument type).

Different strategies for library generation and library searching of electrospray source-CID mass spectra have been developed (Weinmann et al., 1999, 2001a,b; Hough et al., 2000; Bristow et al., 2002), but all are based on the same principles. One or several tune compounds is(are) chosen, for which the electrospray mass spectra are recorded at various acceleration voltages for each instrument. The breakdown curves (relative intensities as a function of the voltage difference between the sampling device and the skimmer) are constructed. The breakdown curves are usually found to have the same overall shape (which indicates a similar time scale on the different instruments), but the *x*-axis (voltage) may be offset from one instrument to another. An example is shown in Figure 4. Usually three different voltages are chosen, corresponding to low, medium, and high fragmentation. The breakdown curves are used to find out the corresponding voltages on the other instruments. This is a relatively simple empirical calibration of the electrospray mass spectra. With this method, three different libraries corresponding

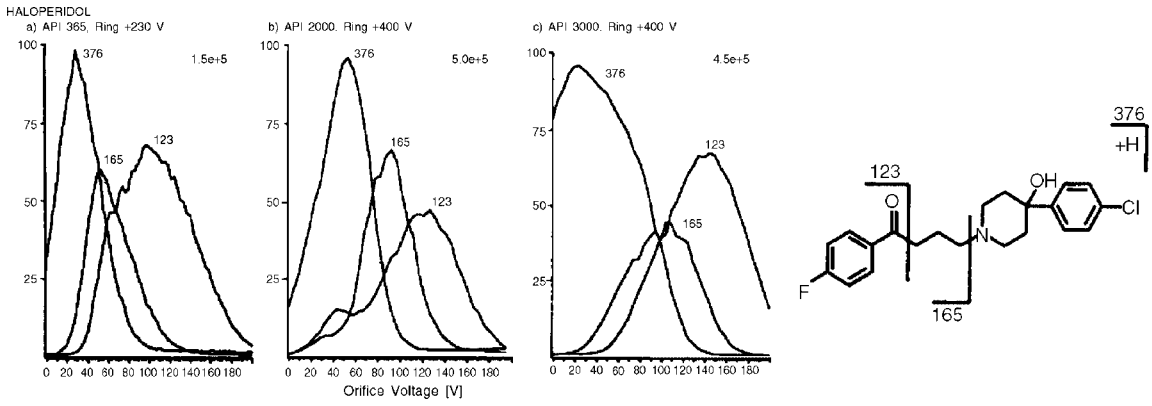


**FIGURE 4.** Chemical structure of haloperidol and breakdown curves from orifice ramping experiments using API 365 (**a**), API 2000 (**b**), and API 3000 (**c**) instruments. (Weinmann W, Stoertzel M, Vogt S, Svoboda M, Schreiber A, Tuning compounds for ESI/in-source CID and mass spectra library searching. J Mass Spectrom 36:1013–1023, Copyright © 2001 John Wiley and Sons. This material is used by permission of John Wiley and Sons.)

to the three different fragmentation conditions have to be built and searched (one for each voltage).

One of the problems is that the voltages that correspond to low, mid, or high fragmentation yields vary with the compound: the fragmentation threshold increases with the mass, so that higher voltage is required to fragment larger ions (Griffin & McAdoo, 1993). To overcome this problem, Lips et al. (2001) used a mass-dependent ramped voltage during the mass scan to generate their drug library. Another important point is that the CID spectra should be highly informative to provide a fingerprint that allows unambiguous compound identification with the library. Marquet et al. (2000), therefore, used a different approach to generate information-rich libraries: for each drug, they recorded a pair of spectra in the positive ion mode in soft and hard conditions (orifice voltages on their API 100: +20 and +80 V), and a pair of negative ion spectra (−20 and −80 V). These reconstructed spectra (sum of the spectra in soft and hard conditions) showed at least as many fragments as MS/MS spectra, and sometimes as many as electron-ionization spectra. Two libraries are generated: one for positive ions and one for negative ions.

For such applications, a experimental calibration of the internal energies of ions produced in different experimental conditions (instrument configuration, voltages, pressure(s), solvent), or better, predictive tools to estimate ion internal energies in given conditions, would be extremely useful.

## B. Non-covalent Complexes

Another field in which source-CID is widely used is for the investigation of non-covalent complexes (Light-Wahl, Schwartz, & Smith, 1994; Ramanathan & Prokai, 1995; Rogniaux et al., 1999; Gabelica et al., 2000; Hunter, Mauk, & Douglas, 2000; Rostom et al., 2000). Source-CID allows the study of very large complexes, even when the *m/z* ratios are too high to be selected for MS/MS (Rostom et al., 2000). The energy necessary to dissociate the complexes is a measure of the gas-phase stability, and is often quantified by a parameter like $V_{50}$, the voltage at which 50% of the complex is fragmented (Rogniaux et al., 1999; Gabelica et al., 2000). An alternative to ''skimmer dissociation'' is ''heated capillary dissociation,'' or HCD, where the dissociation of the complex is monitored as a function of the capillary temperature (Penn et al., 1997b; He et al., 1999; Garcia et al., 2001).

The comparison between source-CID spectra and MS/MS spectra obtained with different fragmentation time and energy ranges gives some clues on the time and energy range accessed in electrospray source-CID. This is shown in Figure 5 for the DNA duplex d(CGCGGGCCCGCG)$_2$, which fragmentation shows an exquisite sensitivity to the internal energy (Gabelica & De Pauw, 2002). Source-CID spectra have been obtained on a Finnigan LCQ mass spectrometer (source configuration: see Fig. 1i), by either increasing the capillary temperature (Fig. 5a), the acceleration because of the tube lens (Fig. 5b), or the voltage difference between the capillary and the skimmer (Fig. 5c). The fragmentation pattern is similar to that obtained in MS/MS on a quadrupole-TOF instrument, whereas quadrupole ion trap MS/MS spectra acquired with the Finnigan LCQ (time scale = 3 ms) show much less direct bond cleavages and much more base loss, which comes from a rearrangement reaction. This suggests that the dissociation time scale in source-CID is below the millisecond. It also suggest that, whatever the source of internal energy (increase of the capillary temperature or collisions between the capillary and the skimmer), the resulting mass spectra are very similar, suggesting that the dissociation takes place on the same time scale. This invalidates the approach for the determination of dissociation thresholds based on the Arrhenius treatment of dissociation rates as a function of the heated capillary temperature. As explained in Section IV-D, this is valid only in the rapid energy exchange limit (limiting case 1), i.e., if the dissociation would take place in the heated capillary only, and much slower than activation and deactivation. The fact that the HCD spectra are similar to the source-CID spectra rather suggest that the

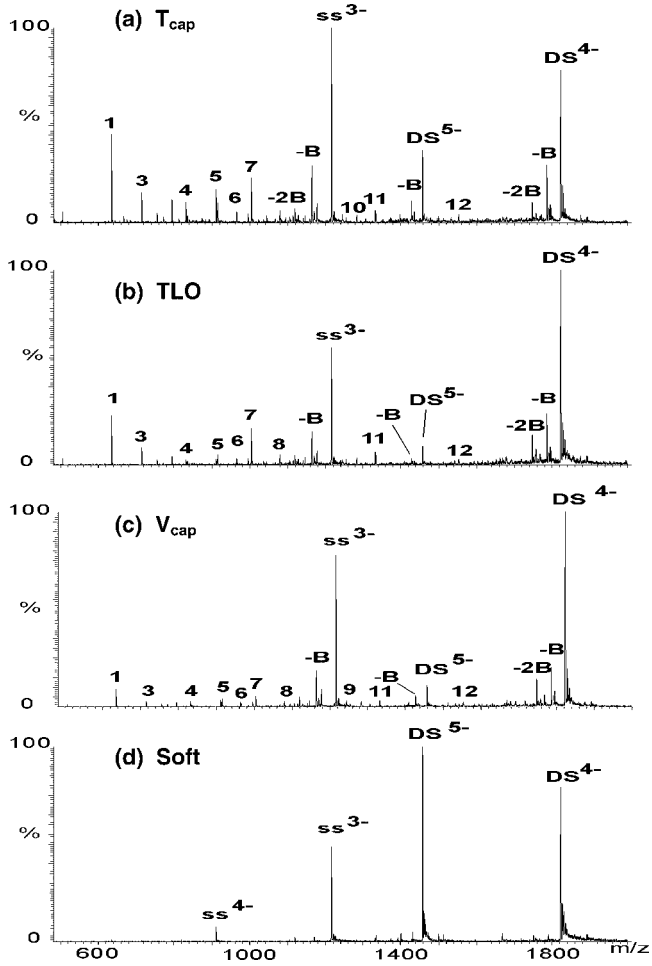


**FIGURE 5.** Full scan MS spectra of duplex d(CGCGGGCCCGCG)$_2$ obtained with a Finnigan LCQ under hard source conditions achieved in three different ways and in soft conditions. **(a)** The capillary temperature is increased to 300°C. **(b)** The tube lens offset is decreased to −30 V. **(c)** The capillary voltage is decreased to −130 V. **(d)** The soft source conditions are: Capillary temperature = 170°C, capillary voltage = −30 V, and tube lens offset = 40 V. DS = double-stranded DNA; ss = single-stranded DNA; −B = neutral base loss from DS or ss; 1 = $w_2^-$; 2 = $a_5$-$B^{2-}$; 3 = $a_3$-$B^-$; 4 = $a_6$-$B^{2-}$; 5 = $w_6^{2-}$; 6 = $w_3^-$; 7 = $a_4$-$B^-$; 8 = $w_7^-$; 9 = $w_8^{2-}$, 10 = $w_4^-$; 11 = $a_5$-$B^-$; 12 = $w_{10}^{2-}$.

dissociation takes place after the ions leave the capillary, and probably after they pass the skimmer (limiting case 2).

### C. Influence of the Energy Received in the Source on the MS/MS Spectra

The literature provides many examples where the nature of the ionization source, or the source-CID conditions do influence the MS/MS spectra. Several studies (Smith & Barinaga, 1990; Kilby & Sheil, 1993; Boschenok & Sheil, 1996) have shown that the higher the acceleration voltage in the source, the lower the collision energy has to be in order to achieve the same fragmentation extent. In other words, unless they are thermalized like in an ion trap analyzer, ions keep a memory of the internal energy they received in the source.

Comparative studies of several ionization sources on a same instrument are also enlightening on their relative hardness/softness. MS/MS spectra of compounds containing long aliphatic chains usually show only even-electron fragments when the ions are produced by particle bombardment methods (LSIMS or FAB), whereas radical fragments show up only for ESI-produced ions (Cheng, Pittenauer, & Gross, 1998; Seto et al., 2001). Bourcier et al. (2001) have shown that 1,4-benzodiazepine ions rearranged when produced by particle bombardment, and not when produced by ESI. Burinsky et al. (2001) have compared the fragmentation of 4-azasteroid and related compounds produced by electrospray and atmospheric pressure chemical ionization (APCI): the MS/MS of dutasteride $[MH]^+$ shows different fragmentation pathways, depending on the source. The authors attribute this behavior to differences in ion populations, either in structure (isomerization) or in internal energy distributions. The usual trend is that the electrospray-produced ions show a higher fragmentation threshold than if produced by other sources. This is attributed to a lower internal energy content in ESI. However, the opposite trend has been observed by Danell & Glish (2001), who showed that peptide ions formed by nanoelectrospray had lower BAD (boundary-activated dissociation in a quadrupole ion trap) thresholds than ions formed by LSIMS. It must, however, been stressed that, in trapping cells like quadrupole ion traps or FTICR cells, ions are thermalized by collisions or photon emission, whereas this is not possible in beam-type instruments because of different pressure and time scale. The lower BAD onsets rather indicate that rearrangement has occurred in LSIMS-produced ions, and that ions were then cooled down to a lower energy minimum in the potential energy surface. In conclusion, compared to ionization techniques like LSIMS, FAB, and APCI, electrospray minimizes ion fragmentation and internal rearrangements, and can be considered as softer.

## VI. DETERMINATION OF INTERNAL ENERGY IN ELECTROSPRAY

### A. Determination of Internal Energy Distributions from the Measured Fragmentation Extent of ''Thermometer'' Ions

As we have seen in Section IV, there is an inter-dependency between (i) the ion dissociation rate, (ii) the ion internal energy $E$ or internal energy distribution $P(E)$, (iii) the time scale of the experiment, and (iv) the relative intensities of the parent and fragment ions. In principle, knowing three of these parameters allows to infer information on the fourth one. For example, in Section IV, we have shown how to calculate the ion intensities by a convolution of the rate constant $k(E)$ by the internal energy distribution $P(E)$. However, mathematically, the deconvolution procedure to infer the function $P(E)$ from the breakdown curves and $k(E)$ is not so simple, because of the fact that both $k(E)$ and $P(E)$ have a complex dependency on both the energy and the time. The simplest way to solve the problem is to characterize either the rate constant or the internal energy distribution by a single parameter instead of their whole distribution as a function of $E$. These procedures and the underlying approximations are described below.

#### 1. The "Survival Yield" Method

The basic assumption in this approach is that all ions having an internal energy below the critical energy $E_0$ do not dissociate (are observed as intact parent ion), whereas all ions having an internal energy above the critical energy do dissociate (are observed as fragments). In other words, the rate constant is supposed to be equal to zero for $E < E_0$ (no dissociation), and infinitely large for $E > E_0$ (complete dissociation). The full dependence of the rate constant on the internal energy is, therefore, characterized by a single parameter: $E_0$. The survival yield ($SY$) of the parent ion $\left[I_M/\left(I_M + \Sigma I_{frag}\right)\right]$ is equal to the fraction of the ions that have an internal energy below the critical energy, i.e., to the integral below the internal energy distribution $P(E)$ from $E = 0$ to $E = E_0$. If the function $SY(E)$ is the integral of the function $P(E)$, then $P(E)$ can be found by derivation of $SY(E)$. One, therefore, needs a single ion, or a set of ions having the same internal energy distribution, having different critical energies. These ions for which the values of $E_0$ are known are often called "thermometer" ions.

This approach has been originally developed in the 1980s (Kenttämaa & Cooks, 1985; Wysocki, Kenttämaa, & Cooks, 1987; Cooks et al., 1990), using thermometer ions which fragment successively via a reaction sequence:

$$M^+ \underset{E_0(1)}{\longrightarrow} F_1^+ \underset{E_0(2)}{\longrightarrow} F_2^+ \underset{E_0(3)}{\longrightarrow} F_3^+ \longrightarrow \cdots$$

The thermometer ions were $(C_2H_5)_4Si^{+\cdot}$, $Fe(CO)_5^{+\cdot}$, and $W(CO)_6^{+\cdot}$, for which the critical energies are known. Tetraethylsilane has been used by Voyksner & Pack (1991) for the determination of internal energy distribution in electrospray. Unfortunately these authors did not mention whether they studied the radical cation or the protonated ion. Indeed, these radical cations as thermometer ions are more suited to EI or photoionization sources.

For the investigation of soft ionization techniques (initially FAB and LSIMS, and later ESI), another set of compounds has been proposed in the early 1990s (De Pauw et al., 1990; Derwa, De Pauw, & Natalis, 1991), consisting of substituted benzylpyridinium salts (Fig. 6). Those compounds have been chosen for their very simple fragmentation mechanism, consisting in the loss of neutral pyridine to give the benzyl cation as the only fragment. As the compounds have similar masses, structures, and

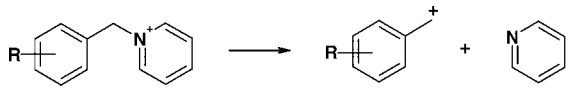

**FIGURE 6.** Structure and fragmentation pathway of the benzylpyridinium cations. (Reprinted with permission from Int J Mass Spectrom 231, Gabelica et al., Influence of the capillary temperature and the source pressure on the internal energy distribution of electrosprayed ions. pp 189–195, Copyright © 2004, with permission from Elsevier.)

number of degrees of freedom, they are supposed to have the same internal energy distribution. For the calculation of the critical energies $E_0$, it is assumed that the fragmentation proceeds without a reverse barrier, which is likely to be the case in such a simple bond cleavage. The critical energies for fragmentation can, therefore, be calculated as the energy difference between the zero-point energy of the products and the zero-point energy of the reactant.

The different substituents are listed in Table 1, together with their corresponding critical energies calculated at different levels of approximation. The critical energy values used in the early studies (De Pauw et al., 1990; Derwa, De Pauw, & Natalis, 1991; Collette et al., 1998; Collette & De Pauw, 1998) are the result of rough calculations and approximations. However, the fragmentation extent in given experimental conditions does not always correlate very well with these critical energy values. The critical energies have been recalculated more recently by AM1 (semi-empirical), *ab initio* HF/6-31G*, and B3LYP/6-31G (DFT). The higher the critical energy, the higher will be the mean internal energies calculated using these values. AM1 and *ab initio* methods give critical energy values with better agreement with the observed survival yields, and the latter is supposed to give more accurate absolute values.

In our most recent study (Gabelica, De Pauw, & Karas, 2004), we used the six para-substituted molecules, with the recalculated AM1 critical energies, for investigating the shape of the internal energy distributions. The advantage of using only para-substituted molecules is that all compounds can be injected simultaneously, which is a guarantee that all survival yields are measured in the same experimental conditions. The masses of the substituents are different enough for the various parent and fragment ions to be distinguished easily. The procedure is illustrated in Figure 7. The survival yields of each molecule are calculated from the relative intensities in the mass spectra (Fig. 7a) and plotted as a function of the critical energy (Fig. 7b). Two more points are added manually, expressing that no parent ion would survive if the critical energy is equal to zero, and that all parent ion would survive if the critical energy is very large. As explained in the first paragraph, the internal energy distribution is obtained by the derivation of $SY(E)$. Not to bias the outcome of the result, the rigorous procedure would be to calculate manually the derivate of these few experimental points, i.e., the coordinates of $P(E)$ are given by Eqs. 10 and 11. N experimental points plus two additional points give $N+1$ points representative of the

**TABLE 1.** Fragmentation critical energies of the benzylpyridinium ions used for the calibration of the internal energies

| R | $E_0$ (eV) as used in initial studies (Collette et al., 1998; Collette & De Pauw, 1998) | $E_0$ (eV) calculated by AM1[c] | $E_0$ (eV) calculated by *ab initio* HF/6-31G* | $E_0$ (eV) calculated by B3LYP/6-31G |
|---|---|---|---|---|
| p-$OCH_3$ | 1.34[a] | 1.51 | 1.40 | 1.86 |
| p-$CH_3$ | 1.60[a] | 1.77 | 1.80 | 2.21 |
| o-$CH_3$ | 1.64[b] | 1.80 | - | 2.29 |
| p-F | 1.80[b] | 1.87 | 1.93 | 2.44 |
| p-Cl | 1.73[a] | 1.90 | 2.04 | 2.44 |
| m-$CH_3$ | 1.65[b] | 1.90 | 1.99 | 2.37 |
| m-$OCH_3$ | 1.68[b] | 1.95 | 2.17 | 2.36 |
| p-CN | | 2.10 | - | |
| p-$NO_2$ | 2.12[a] | 2.35 | - | 2.91 |

[a]Calculated by AM1 with MOPAC (Katritzky et al., 1990).
[b]Calculated by correlation with ionization energies (Derwa, De Pauw, & Natalis, 1991).
[c]Gabelica, De Pauw, & Karas (2004).

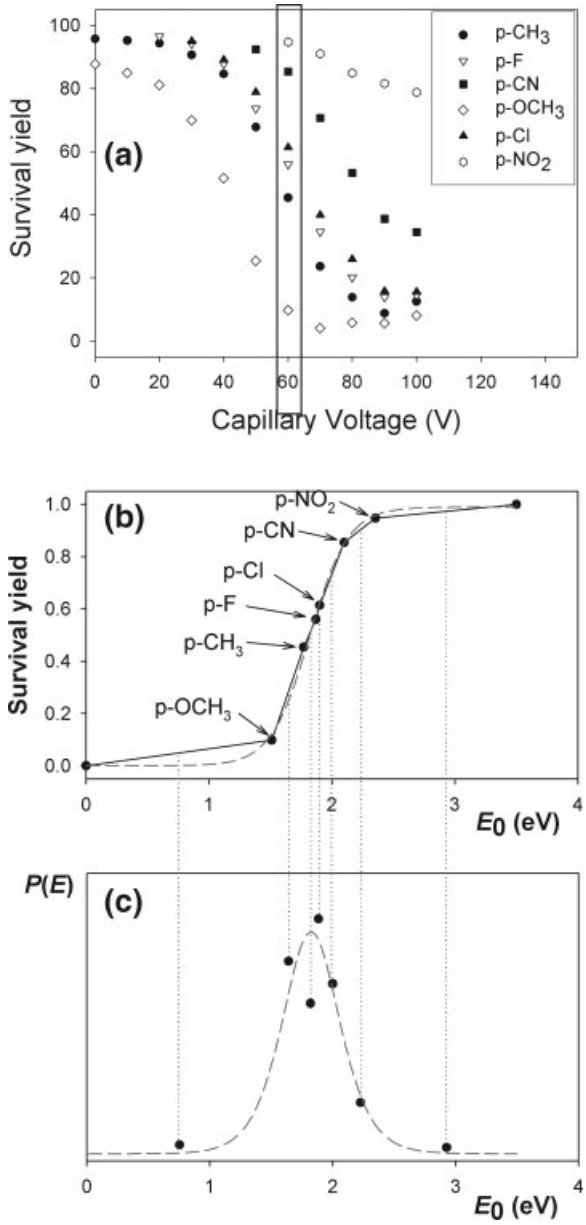


**FIGURE 7.** Calculation of the internal energy distribution with the survival yield method. (**a**) Breakdown curves are recorded as a function of the capillary-skimmer voltage (Finnigan LCQ; solvent: $H_2O$/MeOH 50/50; capillary temperature: 230°C; tube lens offset: −30 V). (**b**) Survival yields at a capillary-skimmer voltage of 60 V as a function of the fragmentation critical energy. The two points with coordinates (0,0) and (1,3.5) have been added manually. Dashed line: Fitting of the points with a sigmoid (3 parameters). (**c**) Internal energy distribution. Filled circles: Derivate of the experimental points in (b). Dashed line: Derivate of the dashed line in (b).

internal energy distribution, as shown in Figure 7c.

$$\text{Ordinate} = [SY(\text{N}+1) - SY(\text{N})]/[E_0(\text{N}+1) - E_0(1)] \quad (10)$$

$$\text{Abscissa} = [E_0(\text{N}) + E_0(\text{N}+1)]/2 \quad (11)$$

Figure 7c shows a very favorable case for which (1) the survival yields rank correctly with the critical energies (otherwise some of the derivates would be negative) and (2) the points are well spread between SY = 0 and 1, and, therefore, the internal energy distribution is well-characterized. It is clear from Figure 7a that, at voltages ≤40 V, or ≥80 V, the internal energy distribution becomes ill-defined. For these two reasons, the derivate is often made not directly from the experimental points, but on a fitting of these experimental points (Collette et al., 1998; Collette & De Pauw, 1998; Collette, Moenen, & De Pauw, 1998), as shown by the dashed lines in Figure 7b,c. While it is clear that the internal energy distribution always presents a gaussian-like overall shape, it must nevertheless be emphasized that the detailed shape of the resulting $P(E)$, especially at the edges, is influenced by the choice of the equation for fitting the survival yields curve, which is an arbitrary choice belonging to the experimentalist.

### 2. *Survival Yield Method Including the Kinetic Shift*

The survival yield method as described above does not take into account the kinetic shift, and is, therefore, not at all quantitative. It must be recognized that, at the critical energy $E_0$, the rate constant is too slow for the reaction to be observed within the time scale of the experiment. Actually higher energies than $E_0$ must be achieved for the fragment to be observed, and true internal energy distributions have a higher mean internal energy than determined by the original survival yield method. A simple way to account for the influence of the kinetic shift has been proposed by Collette et al. (1998): the critical energy $E_0$ is replaced by the appearance energy $E_{app}$, which is the energy at which the rate constant for the dissociation is equal to $1/\tau$, $\tau$ being the time scale of the experiment. This approach, therefore, requires the computation of the rate constants as a function of the internal energy using RRKM equation (Vékey, 1996; Hase, 1998; Steinfeld, Francisco, & Hase, 1999; Lorquet, 2000). It must be noted that this treatment of the kinetic shift is slightly different from its traditional definition, which is usually related to threshold measurements, as explained in Section IV. Nevertheless, this is a convenient method for making the internal energy distribution determination more quantitative.

As a short conclusion on the survival yield method, it is well-suited for the investigation of the shape of the internal energy distributions. It is also well suited to tune experimental conditions on a given instrument. However, the quantitative determination of the mean internal energy depends greatly on the calculation level of the critical energy, and on how accurately the kinetic shift effect is taken into account. The latter requires the determination of $\tau$, by modeling of the ion trajectory in the instrument (see below), and the calculation of $k(E)$ by RRKM method.

### 3. *The "Characteristic Temperature" of Electrosprayed Ions*

Using the "survival yield" method, it has been observed that the internal energy distributions were qualitatively similar to thermal energy distributions (Collette et al., 1998; Collette & De Pauw, 1998). It is, therefore, convenient to characterize the internal energy distribution by a single parameter called the "characteristic temperature." $T_{char}$ is the temperature of the Boltzmann

internal energy distribution which would give the same fragmentation extent as observed experimentally. It is similar to the "effective temperature" concept, but the latter is often associated to the kinetic method (Drahos & Vékey, 1999b; Ervin, 2000). In addition to being mathematically convenient, the characterization of $P(E)$ by a temperature-like parameter is also physically sound. As ionization proceeds at atmospheric pressure, excitation occurs via many collisions. The internal energy distribution produced is often similar to a thermal distribution, despite the fact that the ion is not strictly at thermal equilibrium with a bath gas ($T_{char}$ is different from $T_{gas}$).

Theoretical survival yields are calculated as a function of the temperature using Eq. 12

$$SY(T) = I_M(T)/[I_M(T) + I_F(T)] \quad (12)$$

$I_M(T)$ and $I_F(T)$ are calculated using Eqs. 8 and 9, where $P(E)$ is replaced by the Boltzmann energy distribution at temperature $T$:

$$P(E;T) = \frac{N(E).\exp(-E/k_BT)}{\int_0^\infty N(E).\exp(-E/k_BT).dE} \quad (13)$$

where $N(E)$ is the density of states at the energy $E$, $k_B$ is the Boltzmann constant, and $T$ is the temperature of the Boltzmann energy distribution. The characteristic temperature is the temperature for which the calculated survival yield is equal to the observed survival yield (Drahos et al., 1999).

These equations explicitly take into account the energy dependence of $k(E)$ and the effect of the time scale of the experiment $\tau$. Some refinements can be introduced in the case of quadrupole mass spectrometers, where two different time scales have to be considered. For the parent ion, $\tau$ is the time spent from the skimmer to the exit of the quadrupole, whereas for the fragment ion, $\tau$ is the time spent between the skimmer and the entrance of the quadrupole (respectively, 160 and 80 μs for the benzylpyridinium ions in a VG Platform mass spectrometer). The determination of the ion characteristic temperature does not necessitate a series of probe molecules like in the survival yield method, as a characteristic temperature can be calculated for each ion. This feature allowed to validate one of the hypotheses used in the survival yield method, namely that all benzylpyridinium ions have the same internal energy distribution. It has been shown (Drahos et al., 1999) that these ions had indeed the same characteristic temperature (relative standard deviation of 7.9% on average).

## B. Modeling of Internal Energy Uptake in Electrospray Sources

This section will survey different methods contributing to the calculation of internal energy distributions of ions produced in electrospray sources. The reader is encouraged to refer to the original studies for computational details, and to Section VI-C for a joint discussion of the experimental and the modeling results. It must be stressed that, to date, no publication was found where the supersonic expansion, the ion trajectory calculations and the internal energy transfer have been simultaneously taken into account.

### *1. Supersonic Expansion*

In supersonic expansion, the axial velocity is increased at the expenses of the radial velocities. The translational temperature (characterizing the width of the axial velocity distribution) is very low. Moreover, the first stage of the expansion is isentropic. This means that collisions at the beginning of the expansion cause an equilibration of the translational and internal degrees of freedom (Hayes & Small, 1983). Therefore, the internal energy of the ions diminishes. The effect of the supersonic expansion is, therefore, twofold: (1) it influences the velocity of the ions and of the neutral gas, and must thereby be included in the trajectory calculations and (2) it influences the internal energy of the ions.

Campbell and co-workers (Campbell, Guan, & Laude, 1993) have studied the kinetic energy distributions (which are different from the internal energy distributions) for optimizing the trapping parameters in ESI-FTICR-MS. The final ion velocities depend on the relative contribution of the supersonic expansion and of the acceleration between the orifice and the skimmer. The more the skimmer penetrates into the Mach disk, the more important is the contribution of the acceleration voltage. Hunt et al. (1998) have presented a model and equations accounting for the *m/z* dependence of ion focusing in the source, which are also take into account the supersonic expansion. In their studies on a VG Quattro mass spectrometer, the skimmer lies significantly beyond the Mach disk.

Schneider & Chen (2000) have addressed the supersonic expansion in their modeling of the collision-induced dissociation in the orifice-skimmer region of an electrospray source. In their instrument (a prototype ionspray source from PE Sciex), the skimmer penetrates into the Mach disk, and the role of the expansion is, therefore, very important. Equations are provided which relate the gas number densities to the position relative to the orifice. This allows to calculate the mean free path of the ions and the number of collisions between the orifice and the skimmer. Hoxha et al. (2001) ignored the supersonic expansion, and used a constant mean free path for their modeling of the electrospray source of a VG Platform mass spectrometer. However, with such source design, it has been shown that the skimmer lies beyond the Mach disk (Hunt et al., 1998). As the energetic collisions occur mainly near the skimmer, this approximation seems justified.

The effect of the supersonic expansion on the internal energy distribution of the ions is much less well-characterized than the effect on the ion kinetic energy. The final kinetic temperature attained depend upon the properties of the gas, and on the position relative to the orifice [for equation, see Schneider & Chen (2000)]. As the coupling between the internal and the translational degrees of freedom is not perfect (translation-rotation coupling being more efficient than translation-vibration coupling), the internal temperatures reached in the silent zone are comprised between the translational temperature and the initial temperature, i.e., between 10 K and the source temperature, but are extremely difficult to estimate (Hayes & Small, 1983; Mayer & Baer, 1996). At the level of the shock waves (transition between the silent zone and the exterior), the translational, rotational, and vibrational degrees of freedom are re-randomized by collisions with the bath gas, and the molecules are, therefore, warmed up again to the source temperature.

### 2. Simulation of the Ion Optics

The simplest approximation is to assume a linear field between the orifice and the skimmer (Schneider & Chen, 2000), but this does not seem very realistic because of the cone-shape of the skimmer. A tip effect is much more likely. This tip effect is even enhanced in modern sources containing additional focusing items. However, if the voltage applied is important, the shape of the source electrodes plays an important role as well. The shape of the electrodes defines the electric field gradient and, therefore, the acceleration of the ions. The only way to simulate correctly the ion trajectory is to compute explicitly the ion optics with a program like SIMION (Dahl, 1995) (Scientific Instrument Services, Ringoes, NJ). This has been shown by Hoxha et al. (2001) in the case of the source of a VG Platform (source type: see Fig. 1k). The equipotential lines, shown in Figure 8, exhibit a strong tip effect at the skimmer cone. The major contribution to the acceleration of the ions occurs close to the skimmer cone where the electric field is the strongest.

### 3. Internal Energy Transfer

In a binary collision, the maximal energy available for transfer into internal energy is the relative kinetic energy in the center-of-mass frame of reference ($KE_{COM}$). A simple relationship between the laboratory kinetic energy ($KE_{lab}$) and $KE_{COM}$ is given by Eq. 14:

$$KE_{COM} = \frac{m_n}{m_n + m_i} KE_{tab} \qquad (14)$$

where $m_n$ is the mass of the neutral target gas and $m_i$ is the mass of the ion of interest (McLuckey, 1991; Shulka & Futrell, 1993; Shulka & Futrell, 2000). If the collision is inelastic, part of $KE_{COM}$ is transferred into internal energy (Shulka & Futrell, 2000). The modeling must, therefore, take into account both the increase in internal energy and the decrease in the kinetic energy.

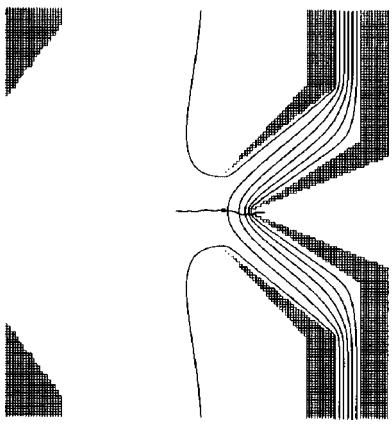

**FIGURE 8.** Geometry of the relevant part of the source of the VG Platform single quadrupole mass spectrometer as simulated by SIMION, equipotential lines, and one representative ion trajectory. (Reprinted with permission from J Phys Chem A 105, Hoxha et al., Mechanism of collisional heating in electrospray mass spectrometry: Ion trajectory calculations. pp 7326–7333, Copyright © 2001 American Chemical Society.)

This can be done either by conducting random walk simulations, as has been done in the two studies relevant to electrospray modeling (Schneider & Chen, 2000; Hoxha et al., 2001), or by master equation modeling, for example with the MassKinetics program (Drahos & Vékey, 2001).

The most difficult parameter to estimate is the fraction of the center-of-mass kinetic energy which is converted into internal energy. The different modes of energy transfer and their relative efficiencies are presented very clearly in the account article of McLuckey (1991). In the experimental conditions encountered in ESI sources, electronic excitation of the ions is usually ignored. Basically two mechanisms can account for the transfer of translational to vibrational energy. The first mechanism is the formation of a long-lived complex between the ion and the target gas. In this case, at each collision, the internal energy of the analyte, the internal energy of the target gas (if not atomic gas) all the relative kinetic energy $KE_{COM}$ are put in common in the complex and redistributed statistically in internal energy and relative translation energy upon dissociation. The energy transfer is very efficient but the long-lived complex model is vadil only for low $KE_{COM}$ values. The second mechanism is called the "impulsive collision mechanism." For large molecules, the collision can be viewed as inelastic with the whole molecule, but as elastic with one subunit. The recoil of that subunit is responsible for the elongation of some bonds and the recoil energy is transferred to vibrational energy that can be subsequently redistributed. The efficiency of this mechanism is typically lower than for the mechanism of complex formation, but it is favored at higher $KE_{COM}$.

Schneider & Chen (2000) used the crude approximation that all the center-of-mass kinetic energy was converted into internal energy. Hoxha et al. (2001), however, used the long-lived collision complex model to calculate the mean fraction of the $KE_{COM}$ converted into internal energy. This fraction $f$ decreases with the fraction of the number of degrees of freedom which are in the gas, and with the lifetime of the complex (which increases with the depth of the interaction potential energy well, with the number of degrees of freedom of the complex and decreases with $KE_{COM}$) (McLuckey, 1991). The long-lived complex model, where the energy is re-randomized at each collision, accounts for both activating and deactivating collisions. A consequence is that Boltzmann-like internal energy distributions are reached after a few collisions (Drahos & Vékey, 2001; Hoxha et al., 2001), which is in agreement with the observed shape of the internal energy distributions, as determined using the survival yield method (see above).

## C. Internal Energy of Electrospray-Produced Ions: Results

### 1. Influence of the Orifice-Skimmer Voltage Difference

Qualitatively, it is obvious that the internal energy of the ion increases when the acceleration potential between the orifice and the skimmer increases, whatever the source configuration. Let us examine how the experimental and modeling methods described above can give some insight into the quantitative aspects of this process.

Both Voyksner & Pack (1991) and Collette & De Pauw (1998) have shown that, upon increasing the orifice-skimmer voltage, the internal energy distributions become wider and are shifted towards higher energies. In these two studies, the mean internal energy was calculated directly from the internal energy distributions. Voyksner and Pack found that the mean internal energy increases roughly linearly with the capillary-skimmer voltage of their source (Analytica of Brandford). However, in the study of Collette et al. (1998) on the ESI sources of a VG Platform and a PE Sciex API 165 instrument, the mean internal energy was found to increase faster than linearly with the acceleration voltage. In a later study by Drahos et al. (1999), it is shown that it is rather $T_{char}$ which is linearly proportional to the voltage (Fig. 9). The mean internal energy is related to the temperature by equations by Vékey (1996) and Drahos & Vékey (1999a):

$$\langle \mathrm{E} \rangle = c(T, \upsilon).s.k_{\mathrm{B}}.T \tag{15}$$

where $s$ is the number of oscillators, $k_B$ is the Boltzmann constant, $T$ the temperature, and $c(T,\upsilon)$ the heat capacity of the molecule, which depends on the vibrational frequencies and on the temperature. The dependency on the temperature can be approximated by Drahos & Vékey (1999a):

$$c(T, \upsilon) = \mathrm{aT} + \mathrm{bT}^2 \tag{16}$$

The linear relationship between the internal temperature and the acceleration voltage can be understood in the framework of the equilibration between the internal and the translational degrees of freedom. This is possible only if many collisions occur between the ion and the bath gas, and if collisional activation and deactivation are considered. Then the characteristic (or 'effective') internal temperature is equal to the effective translational temperature (Hoxha et al., 2001), or at least directly proportional to it (Raznikov et al., 1999). This model has also been used to characterize the energy uptake in quadrupole ion trap resonant excitation, which is also characterized by multiple low-energy collisions (Goeringer & McLuckey, 1996a,b). The kinetic energy in the center-of-mass frame of reference is related to the effective translation temperature by:

$$KE_{\mathrm{COM}} = 3/2.k_{\mathrm{B}}.T_{\mathrm{eff,transl}} \tag{17}$$

As a consequence,

$$\begin{aligned} T_{\mathrm{char,int}} &\propto KE_{\mathrm{COM}} \propto [m_{\mathrm{n}}/(m_{\mathrm{n}} + m_{\mathrm{i}})].\, KE_{\mathrm{lab}} \\ &\propto [m_{\mathrm{n}}/(m_{\mathrm{n}} + m_{\mathrm{i}})].V \end{aligned} \tag{18}$$

This explains both the linear relationship between $T_{char}$ and $V$, and also the effect of the number of degrees of freedom on the slope (see the comparison between benzylpyridinium ions and leucine enkephalin in Fig. 9). In such a model taking into account the de-activation process, less energy is transferred to the ion than $KE_{COM}$, or than a constant fraction of $KE_{COM}$ (Drahos & Vékey, 2001). Schneider & Chen (2000), who assumed that all $KE_{COM}$ was converted into internal energy at each collision, predicted a linear relationship between $\langle E_{int} \rangle$ and the voltage. In conclusion, regarding the dependence of the internal energy on the acceleration voltages, the few studies to date are in contradiction, but these studies have been conducted with two different sources (one with the skimmer penetrating into the silent zone, and one with the skimmer beyond the Mach disk). More experiments joined with more accurate modeling studies are, therefore, needed to reach a consensus.

Last but not least, an interesting point in Figure 9 is the characteristic temperature extrapolated at zero acceleration voltage (Drahos et al., 1999; Takats et al., 2002). The authors checked the validity of the parameters used in the calculation of $T_{char}$ by comparison with activation in a thermalized FTICR cell. The characteristic temperatures can be considered to approach closely the true ion temperature. As the skimmer lies beyond the Mach disk, a characteristic temperature close to the source temperature would have been expected: as no external acceleration is applied, the ions should be thermalized by the surrounding gas. This temperature extrapolated at zero voltage could indicate either that the droplet is unexpectedly hot when the naked ion is released (without presuming of the ion production mechanism), or in the case of the ion evaporation mechanism, that the Coulombic repulsion between the ion and the charged droplet provides kinetic energy to the ions, which is subsequently converted into internal energy by collision with the bath gas (Takats et al., 2002).

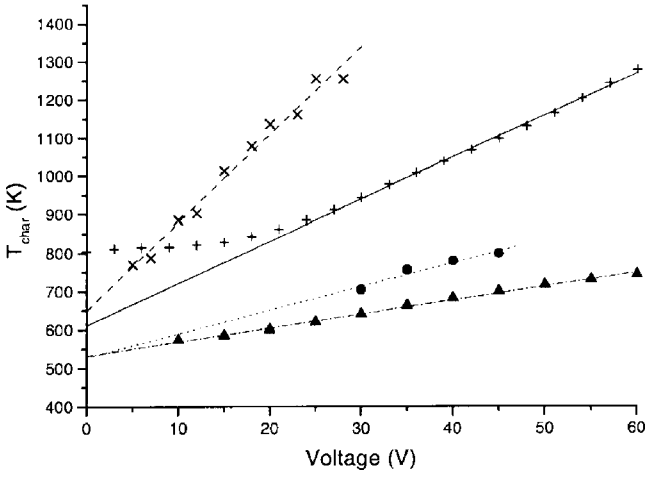


**FIGURE 9.** Characteristic temperatures of benzylpyridinium salts (average for all six compounds) obtained on a PE-SCIEX API 165 (solid line, +) and on a VG Platform (dashed line, ×) by varying the cone voltage. The same experiment was performed in the case of leucine enkephalin on the PE-SCIEX instrument (dashed-dotted line, ▲) and on the VG Platform (dotted line, ●). (Drahos L, Heeren RMA, Collette C, De Pauw E, Vékey K, Thermal energy distributions observed in ESI. J Mass Spectrom 34:1373–1379, Copyright © 1999 John Wiley and Sons. This material is used by permission of John Wiley and Sons.)

## 2. *Influence of the Capillary Temperature*

As mentioned above, in heated capillary ion sources an increase of the capillary temperature causes an increase of the fragmentation extent, all source voltages being kept constant. Another important parameter that can be modulated by the capillary temperature is the extent of droplet evaporation or ion desolvation achieved before the acceleration in the capillary-skimmer region. Recent experiments (Gabelica, De Pauw, & Karas, 2004) have shown that the impact of desolvation on the shape of the

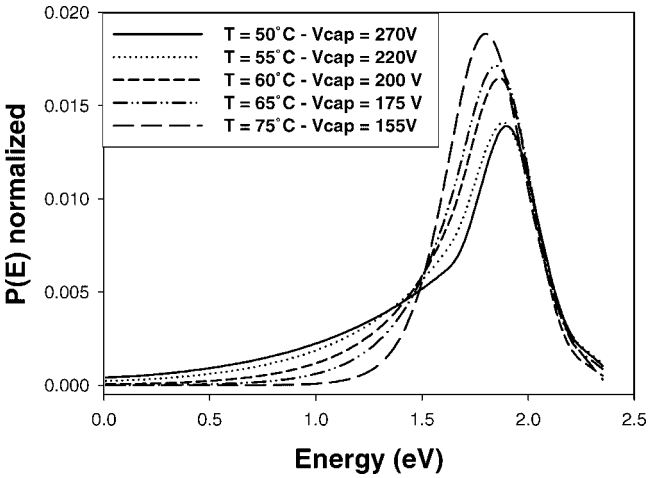


**FIGURE 10.** Influence of the capillary temperature on the shape of the internal energy distributions. Experiments were performed on a Mariner o-TOF instrument with a modified nanospray source including a heated transfer capillary (Schmidt, Bahr, & Karas, 2001). The source pressure was maintained constant. The solvent used was water/methanol (50:50). The different distributions correspond to experimental conditions which all give the same survival yield (0.63) for the *p*-fluoro-benzylpyridinium ion. (Reprinted with permission from Int J Mass Spectrom 231, Gabelica et al., Influence of the capillary temperature and the source pressure on the internal energy distribution of electrosprayed ions. pp 189–195, Copyright © 2004, with permission from Elsevier.)

internal energy distribution is significant. At low capillary temperatures, where a higher voltage is needed to achieve the same fragmentation extent (or survival yield) for a given molecule, the internal energy distribution becomes broader, with clearly a low-energy tail (Fig. 10). The fact that a significant fraction of the ion population has a low energy, and, therefore, can survive without fragmentation even at high voltages, indicates that desolvation was not complete upon arrival in the capillary-skimmer region. Therefore, some ions have undergone many collisions and can fragment within the time scale of the instrument, whereas others have not yet desolvated completely. A consequence of this kind of observation is that approximating the internal energy distribution by a Boltzmann distribution may not always be valid.

### *3. Influence of the Nature and the Pressure of the Collision Gas*

The nature of the collision gas, for given source settings, can also shift the internal energy distribution of the ions (Fig. 11). However, this effect depends greatly on the source design, as explained below. Simple kinematics predict that, for a given laboratory kinetic energy (a given voltage), the center-of-mass kinetic energy, and, therefore, the amount of energy available for conversion into internal energy, increases with the mass of the target gas (Eq. 14). Therefore, the fragmentation extent increases with the mass of the target gas (Douglas, 1982). Although this is the usually observed trend (Collette & De Pauw, 1998; Schmidt, Bahr, & Karas, 2001), the opposite can also be observed when the collision gas undergoes condensation in the supersonic expansion and when the skimmer penetrates into the silent zone

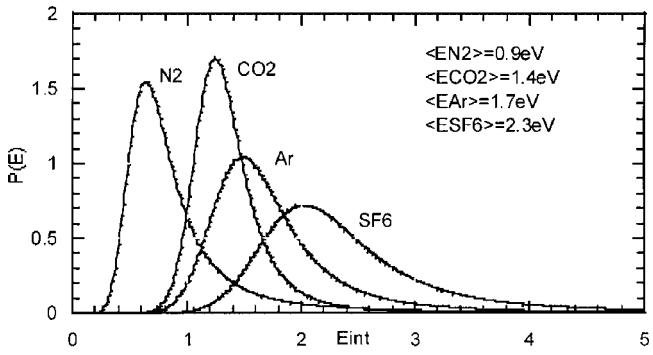


**FIGURE 11.** Internal energy distributions obtained for different collision gases for 15 V on the sampling cone (VG Platform instrument) and water/acetonitrile (50:50) as mobile phase. (Collette C, De Pauw E, Calibration of the internal energy distribution of ions produced by electrospray. Rapid Commun Mass Spectrom 12:165–170, Copyright © 1998 John Wiley and Sons. This material is used by permission of John Wiley and Sons.)

(Schneider, Douglas, & Chen, 2001). In addition to its mass, the number of degrees of freedom of the gas influences the fragmentation extent. This is obvious in the comparison between argon and $CO_2$ in Figure 11. The larger the number of gas DOF, the larger the fraction of $E_{COM}$ which ends up in the gas (and, therefore, not in the ion) upon collision (Collette & De Pauw, 1998; Hoxha et al., 2001; Takats et al., 2002).

In addition to the nature of the gas, its pressure is also a very important parameter, as shown by Schmidt and co-workers (Schmidt, Bahr, & Karas, 2001), who introduced a gas directly in the capillary-skimmer region of their home-made heated capillary nanoelectrospray source. Increased pressure was found particularly useful in the case of sugars or non-covalent complexes, to facilitate desolvation without provoking extensive fragmentation. In their evaluation of the reproducibility of source-CID mass spectral libraries, Bristow et al. (2002) noticed that, on some sources, high infusion flow rates resulted in lower fragmentation extent, and attributed this to an increase of the partial pressure in the source.

Again this effect comes from the concomitance of the droplet evaporation and the ion activation processes. Indeed, a fraction of the ion population may be already fully desolvated (a collision at this stage will thereby cause ion activation), whereas another fraction may still be included in droplets (a collision will likely cause solvent evaporation). In terms of $P(E)$, this translates into a low-energy tail as shown in Figure 10. An increase of the gas pressure in the orifice-skimmer region induces a reduction of the ion mean free path. As the ions are slowed down by inelastic collisions, the mean ion kinetic energy is reduced when the pressure is increased. Schmidt, Bahr, & Karas (2001) suggested that the ions undergo more numerous, but less energetic collisions with the gas. In terms of $P(E)$, this would translate into a narrower internal energy distribution. To prove this hypothesis, Gabelica, De Pauw, & Karas (2004) studied the shape of the internal energy distributions using benzylpyrdinium ions in the same instrument where the source pressure can be varied. A capillary temperature of 50°C was used to start with a $P(E)$ having a low-energy tail. The effect of increasing the source pressure is shown in Figure 12.

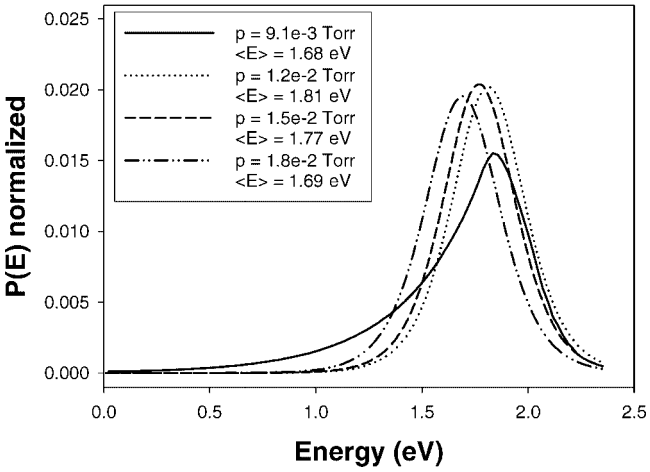


**FIGURE 12.** Influence of the source pressure on the internal energy distributions. Experiments were performed on a Mariner o-TOF instrument with a modified nanospray source including a heated transfer capillary (Schmidt, Bahr, & Karas, 2001). The capillary temperature was 50°C and the capillary voltage at 200 V in all experiments. The solvent used was water/methanol (50:50). The pressure given in the legend corresponds to the pressure measured in the first pumping stage, and is proportional to the source pressure. (Reprinted with permission from Int J Mass Spectrom 231, Gabelica et al., Influence of the capillary temperature and the source pressure on the internal energy distribution of electrosprayed ions. pp 189–195, Copyright © 2004, with permission from Elsevier.)

A small increase of the source pressure suppresses the low-energy tail of the distribution, thereby increasing the mean internal energy and rendering the distribution more thermal-like. This indicates more efficient desolvation. Further increase of the pressure shifts the distribution towards lower energies, maintaining the thermal-like shape. This second effect is because of the lower mean kinetic energy of the ions when the mean free path is reduced.

### *4. Influence of the Solvent*

There is only one report (Collette & De Pauw, 1998) on the influence of the solvent on the internal energy distribution. The authors compared the $P(E)$ obtained with the same instrumental settings for the benzylpyridinium ions in water/methanol and in water/glycerol (90:10). Glycerol has a lower vapor pressure than water, and droplets will be enriched in glycerol upon evaporation. The internal energy distribution is shifted to higher energies when glycerol is used in the mobile phase (Fig. 13). Several hypotheses can explain this observation. (1) The internal energy of the ions may depend on the temperature of the droplet at the moment the ions are emitted in the gas phase. Droplet evaporation is caused by friction when the droplets are drifted by the electric field through the gas at atmospheric pressure. As glycerol requires higher energy for evaporation, the droplets will be hotter when glycerol is added in the mobile phase. (2) The glycerol layer at the surface of the droplets may change the ion ejection dynamics (in the framework of the IEM), and give a higher kinetic energy to the ejected ions, which will undergo more energetic collisions with the gas. The range of mobile

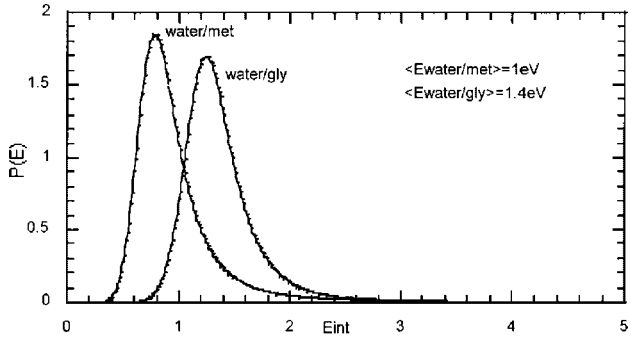


**FIGURE 13.** Internal energy distributions obtained using water/methanol (90:10) or water/glycerol (90:10) with nitrogen as collision gas and 15 V on the sampling cone (VG Platform instrument). (Collette C, De Pauw E, Calibration of the internal energy distribution of ions produced by electrospray. Rapid Commun Mass Spectrom 12:165–170, Copyright © 1998 John Wiley and Sons. This material is used by permission of John Wiley and Sons.)

phases is, however, limited by their ease of application in routine HPLC and ESI.

## D. Comparison with Other ''Soft'' Ionization Sources

### *1. Particle Bombardment*

This discussion concerns ionization methods where secondary ions are emitted from liquid matrices after the bombardment of ions (liquin secondary ion mass spectrometry, LSIMS) or atoms (FAB). The ''survival yield'' method was used for the estimation of the internal energies of secondary ions in LSIMS (Derwa & De Pauw, 1989; De Pauw et al., 1990; Derwa, De Pauw, & Natalis, 1991). However, the direct comparison with electrospray is difficult because the kinetic shift was not taken into account in these early studies. The best way to compare ESI to particle bombardment methods is to compare the fragmentation extent of a given molecule obtained on a single instrument which can be equipped with both sources. In the single MS spectra, it is generally observed that ions produced by electrospray undergo less fragmentation than when produced by FAB or LSIMS (Griffiths et al., 1996; Melnyk et al., 1998). The nature of the liquid matrix was found to have an influence on the fragmentation extent, *m*-nitrobenzylalcohol being softer than thioglycerol (Takayama et al., 1990). Similarly, MS/MS spectra on electrospray or particle bombardment-produced ions suggest that ESI minimizes both fragmentation and isomerization (see Section V-C for the detailed discussion). It appears doubtless that ion internal energies are lower in electrospray than in particle bombardment methods.

### *2. Atmospheric Pressure Chemical Ionization (APCI)*

In APCI, the solution vaporization is assisted by a strong gas flow and high temperatures (in the order of 500°C), but no high voltage is applied. Ionization is produced by an electric discharge in the

source. Similarly to particle bombardment methods, it was found that the internal energy of ions is higher in APCI than in ESI, resulting in lower fragmentation thresholds in MS/MS (Harrison, 1999a), or in isomerization (Burinsky et al., 2001).

### *3. Matrix-Assisted Laser Desorption/Ionization (MALDI)*

The problem of MALDI is more complicated, and the reader is encouraged to refer to recent review articles for a thorough discussion of the desorption and ionization mechanisms (Zenobi & Knochenmuss, 1998; Dreisewerd, 2003; Karas & Krüger, 2003; Knochenmuss & Zenobi, 2003). We will focus here on the points relevant to the comparison with ESI. There are clearly different sources of energy in MALDI, and the matrix plays a determinant role in the various energy transfer processes. Fast fragmentation is often referred to as ''in-source decay'' (ISD) (Brown & Lennon, 1995; Brown, Carr, & Lennon, 1996), with time constants on the order of the phase transition process. Subsequent supersonic expansion induces internal energy cooling of the analyte. In the framework of a 'thermal' desorption model, the internal temperature of the analyte will depend on the phase-transition temperature (or sublimation temperature) of the matrix (Mowry & Johnston, 1994; Thierolf, Bahr, & Karas, 1997), and on possible bottlenecks in the internal energy transfer from the matrix to the analyte (Vertes, Irinyi, & Gijbels, 1993). Glückmann & Karas (1999) suggested that the matrix softness could be correlated with its initial velocity, indicating internal energy cooling upon expansion. The key point is, therefore, the balance between the energy required to separate the analyte from its matrix shell and the internal excitation of the analyte. This recalls the effect of adding glycerol to the mobile phase in ESI. In addition to fast-forming fragments, metastable fragments are also observed, and this process is referred to as ''post-source decay'' (PSD) (Spengler, Kirsch, & Kaufmann, 1992; Kaufmann, Kirsch, & Spengler, 1994; Spengler, 1997). In this case, the internal energy input probably comes from collisions with the matrix plume and/or residual gas upon acceleration. By analogy to ESI, this can be compared with source-CID, but in MALDI-TOF instruments operated in vacuum, collisions with the matrix are more likely than collisions with residual gas.

Luo and co-workers (Luo, Marginean, & Vertes, 2002) recently reported the first quantification of ion internal energies produced by MALDI, by applying the survival yield method using benzylpyridinium ions. Assuming a fragmentation time of 100 ns, the authors found mean ion internal energies of 3.7 eV for CHCA, 4.0 eV for SA, and 4.3 eV for DHB. To make comparisons easier, this corresponds to characteristic temperatures of 1180, 1235, and 1295 K, respectively. The benzylpyridinium thermometer ions were also used by Greisch et al. (2003), who characterized the ion internal energy by an effective temperature instead of an effective energy, but the matrices used are not typical of MALDI conditions. The effective temperatures were around 1360 and 1490 K for $NaNO_3$ and $NH_4CO_3$, respectively. In a recent study (Gabelica, Schulz & Karas, in press), we used the benzylpyridinium to determine the characteristic temperatures in atmospheric pressure MALDI. The lowest characteristic temperature found was in the order of 800 K (using sinapinic acid as the matrix). All these studies show that the internal energy of ions produced in MALDI is higher than in ESI. This correlates well with the significantly higher fragmentation extent observed for gangliosides by ESI-FTMS and MALDI-FTMS on the same instrument (Penn et al., 1997a). The MALDI-FTMS instrument configuration implies longer fragmentation time scales than MALDI-TOFMS, and is, therefore, very sensitive to metastable fragmentation.

### *4. Sonic Spray*

Several other source designs have been explored, with the aim of transferring intact weak non-covalent associations in the gas phase. Recently, the observation of amino acid clusters using ''sonic spray'' has been reported (Takats et al., 2003). The sonic spray source (Hirabayashi, Sakairi, & Koizumi, 1994, 1995; Hirabayashi et al., 1998) employs an extremely high nebulizing gas flow rate, but no voltage difference is applied between the capillary and the counter-electrode. The formation of charged droplets is attributed to statistical charge distribution during droplet formation. Takats et al. (2003) compared the performance of a sonic spray source and an electrospray source, both coupled to a quadrupole ion trap mass spectrometer, using the same instrumental settings. The sonic spray source was found to be softer than the electrospray in terms of formation of intact clusters. The major difference between the two ionization methods resides in the charge density of the droplets. In electrospray, the concentration of excess charge (Enke, 1997) on a droplet is much higher than in sonic spray. In the latter, the Rayleigh limit is not likely to be reached, and shrinkage of the droplet until complete evaporation (charged residue mechanism) is supposed to occur (Takats et al., 2003). This may be the origin of the softness of sonic spray.

### *5. Cold-Spray*

Another source type that has been developed for the analysis of thermally labile assemblies is the ''cold-spray'' ionization source (Sakamoto et al., 2000). In this case, both the sample probe (inlet capillary) and the desolvation chamber are cooled down ($-80$ to $10^{\circ}C$). This source is especially useful for those species which are not stable in solution at room temperature, like e.g. AT-rich DNA complexes (Sakamoto & Yamaguchi, 2003) or Grignard reagents (Sakamoto, Imamoto, & Yamaguchi, 2001). The source can be operated in electrospray mode (with a high voltage on the capillary) and in the sonic spray mode (no voltage) (Sakamoto et al., 2003). While in this source, the internal energy of the system before the ionization process is minimized, whether the final energy of the fully desolvated ions is different from that obtained in the corresponding electrospray or sonic spray conditions has not yet been addressed. For very fragile species, the authors used experimental conditions where the analyte is still partially solvated (Sakamoto et al., 2000; Sakamoto, Imamoto, & Yamaguchi, 2001; Sakamoto & Yamaguchi, 2003).

### *6. Laser Spray*

Hiraoka and co-workers (Hiraoka, Matsushita, & Hukasawa, 1997; Hiraoka et al., 1998; Kudaka et al., 2000) have developed an experimental setup, called ''laser spray,'' in which a IR laser

beam ($CO_2$ laser; 10.6 μm) is fired on the spray. This enhances solvent evaporation and was reported to increases the ion signal. The gain in softness compared to conventional electrospray has not yet been evaluated. It is likely to depend on the balance between solvent activation (and consequently evaporation), analyte activation and energy transfer between the analyte and the solvent.

### *7. Laser-Induced Liquid Beam Ionization/Desorption (LILBID)*

Brutschy et al. have developed a method based on this principle, called laser-induced liquid beam ionization/desorption, or LILBID (Kleinekofort, Avdiev, & Brutschy, 1996; Sobott et al., 1998; Wattenberg et al., 1999). The desorption of the ions from a neutral liquid beam is induced by an IR laser pulse with the wavelength tuned to a strong absorption band of the liquid, i.e., 2.5–3.5 μm (2800–4000 $cm^{-1}$) for water. The solvent undergoes a phase transition followed by expansion. During expansion most of the analytes will be ejected as neutral ion pairs, but a small fraction will remain separated from its counter-ions and will be detected as charged species. The efficiency of separation of ion pairs increases with the dielectric constant of the solvent. The internal energy imparted to LILBID ions has not been quantified yet, but the methods seems promisingly soft: its ability to produce intact non-covalent complex has been demonstrated (Kleinekofort et al., 1996, 1997; Wattenberg et al., 2000; Wattenberg, Sobott, & Brutschy, 2000).

## VII. CONCLUSION AND PERSPECTIVE

It becomes clear that, whatever the ionization method, the internal energy imparted to the analyte depends on two factors: (1) the minimal energy that must be given to separate the analyte from its matrix (volatile solvent in ESI, liquid matrix in FAB/LSIMS, crystalline matrix in MALDI), from its counter-ions, and from possible contaminants, and (2) the subsequent collisions of the naked analyte in the source (in the orifice-skimmer region in ESI, with the plume in MALDI, etc. . .). While the latter can easily be controlled by adjustment of the experimental conditions, the former is inherent to the ionization method. We also already mentioned that these two processes are sometimes not decoupled in time and in space, and a fraction of the analyte population can be already desolvated whereas another is still embedded in a matrix shell.

On the fundamental point of view, the study of internal energy and internal energy distributions is a tool which allows to probe the mechanism by which the analyte is separated from its matrix shell and ionized. In that respect, the nature of the matrix is crucial: the matrix should be easily vaporized/sublimed, and the chemical interactions with the analyte should not be too strong (else the remaining matrix molecules would be difficult to separate from the analyte). As a result, the choice of the matrix should be driven by the nature of the analyte. On the ion internal energy in ESI or in MALDI are just beginning to emerge. To our opinion, further studies in that direction will hopefully give a better understanding of the ionization process (for electrospray as well as for other ionization sources), and eventually to the rational design of new matrices and/or additives for specific applications.

Another fundamental issue in close relationship with the matrix effect is the on-going debate on the ion production mechanism, i.e., the charged residue model versus the ion evaporation model. But if the difference in ion internal energy is indicative of differences in the ion production mechanism (CRM vs. IEM), then ion internal energy measurements could be a probe of the ion formation mechanism. Further studies on the internal energy of ions produced by sonic spray, where the CRM is the only possible ionization route, would be enlightening.

While for some applications ionization conditions must be as soft as possible, for some others, a certain degree of internal excitation is needed to induce fragmentation on purpose. The easiest procedure is to use collision-induced dissociation. This can be realized in normal MS/MS, and we have seen that for beam-type instruments, the energy received in the source has an influence on the MS/MS spectra. CID can also be realized in the source itself, by acceleration in the orifice-skimmer region. A calibration of the ion internal energy as a function of the experimental conditions (acceleration voltage, nature and pressure of the collision gas) could possibly allow energy-resolved measurements to be achieved, either to generate standardized mass spectral libraries, or for thermochemical studies.

## ACKNOWLEDGMENTS

The authors acknowledge the FNRS (Fonds National de la Recherche Scientifique, Belgium) and the University of Liège for supporting the acquisition of the instrumentation. V.G. is thankful to the FNRS (Fonds National de la Recherche Scientifique, Belgium) for a postdoctoral research fellowship and to the Alexander von Humboldt foundation for sponsoring a research stay in Germany. This research has been supported by the ARC (Actions de Recherche Concertées/Communauté Française de Belgique). F. Rosu, JF. Greisch and Dr. G. Dive are acknowledged for recalculating some of the critical energies in Table 1.

## REFERENCES

Amad MH, Cech NB, Jackson GS, Enke CG. 2000. Importance of gas-phase proton affinities in determining the electrospray ionization response for analytes and solvents. J Mass Spectrom 35:784–789.

Baer T, Mayer PM. 1997. Statistical Rice Ramsperger Kassel Marcus quasi-equilibrium theory calculations in mass spectrometry. J Am Soc Mass Spectrom 8:103–115.

Bogusz MJ, Maier R-D, Krüger KD, Webb KS, Romeril J, Miller ML. 1999. Poor reproducibility of in-source collisional atmospheric pressure ionization mass spectra of toxicologically relevant drugs. J Chromatogr A 844:409–418.

Boschenok J, Sheil MM. 1996. Electrospray tandem mass spectrometry of nucleotides. Rapid Commun Mass Spectrom 10:144–149.

Bourcier S, Hoppilliard Y, Kargar-Grisel T, Pechiné JM, Perez F. 2001. Do thermally labile 1,4-benzodiazepines rearrange under electrosrpay and particle bombardment? Eur J Mass Spectrom 7:359–371.

Bristow AWT, Nichols WF, Webb KS, Conway B. 2002. Evaluation of protocols for reproducible electrospray in-source collisionally induced dissociation on various liquid chromatography/mass spectrometry instruments and the development of spectral libraries. Rapid Commun Mass Spectrom 16:2374–2386.

Brown RS, Carr BL, Lennon JL. 1996. Factors that influence the observed fast fragmentation of peptides in MALDI. J Am Soc Mass Spectrom 7:225–232.

Brown RS, Lennon JL. 1995. Sequence-specific fragmentation of MALDI-desorbed protein/peptide ions. Anal Chem 67:3990–3999.

Bruins AP. 1997. ESI source design and dynamic range considerations. In: Cole RB, editor. Electrosrpay ionization mass spectrometry, Chapter 3. New York: John Wiley & Sons. pp 107–136.

Burinsky DJ, Williams JD, Thornquest AD, Sides SL. 2001. Mass spectral fragmentation reactions of a therapeutic 4-azasteroid and related compounds. J Am Soc Mass Spectrom 12:385–398.

Busman M, Rockwood AL, Smith DL. 1992. Activation energies of gas phase dissociations of multiply charged ions from electrospray ionization mass spectrometry. J Phys Chem 96:2397–2400.

Campargue R. 1984. Progress in overexpanded supersonic jets ans skimmed molecular beams in free-jet zones of silence. J Phys Chem 88:4466–4474.

Campbell VL, Guan Z, Laude DA. 1993. Selective generation of charge dependent independent ion energy distributions from a heated capillary electrospray source. J Am Soc Mass Spectrom 5:221–229.

Cech NB, Enke CG. 2001. Practical implications of some recent studies in electrospray ionization fundamentals. Mass Spectrom Rev 20:362–387.

Cheng C, Pittenauer E, Gross ML. 1998. Charge-remote fragmentations are energy-dependent processes. J Am Soc Mass Spectrom 9:840–844.

Chowdhury SK, Katta V, Chait BT. 1990. An electrospray ionization mass spectrometer with new features. Rapid Commun Mass Spectrom 4: 81–87.

Cole RB. 2000. Some tenets pertaining to electrospray ionization mass spectrometry. J Mass Spectrom 35:763–772.

Collette C, Moenen F, De Pauw E. 1998. On the determination of ion internal energy in an electrospray source. In: Nato ASI Series. Vol. 510. New methods for the study of biomolecular complexes. Kluwer Academic Publishers, pp 157–169.

Collette C, De Pauw E. 1998. Calibration of the internal energy distribution of ions produced by electrospray. Rapid Commun Mass Spectrom 12: 165–170.

Collette C, Drahos L, De Pauw E, Vékey K. 1998. Comparison of the internal energy distributions of ions produced by different electrospray sources. Rapid Commun Mass Spectrom 12:1673–1678.

Cooks RG, Ast T, Kralj B, Kramer V, Zigon D. 1990. Internal energy distributions deposited in doubly and singly charged tungsten hexacarbonyl ions generated by charge stripping, electron impact, and charge exchange. J Am Soc Mass Spectrom 1:16–27.

Dahl D. 1995. SIMION 3D. Proceedings of the 43th ASMS Conference on Mass Spectrometry and Allied Topics. 717.

Danell AS, Glish GL. 2001. Evidence for ionization-related conformational differences of peptide ions in a quadrupole ion trap. J Am Soc Mass Spectrom 12:1331–1338.

De Pauw E, Pelzer G, Marien J, Natalis P. 1990. Internal energy distribution of ions emitted in secondary ion mass spectrometry. Org Mass Spectrom 25:103–108.

Derwa F, De Pauw E, Natalis P. 1991. New basis for a method for the estimation of secondary ion internal energy distribution in ''soft'' ionisation techniques. Org Mass Spectrom 26:117–118.

Derwa F, De Pauw E. 1989. Evaluation of internal energy of secondary ions in LSIMS. Spectros Int J 7:227–232.

Dole M, Mack LL, Hines RL. 1968. Molecular beams of macroions. J Chem Phys 49:2240–2249.

Douglas DJ. 1982. Mechanism of the collision-induced dissociation of polyatomic ions studied by triple quadrupole mass spectrometry. J Phys Chem 86:185–191.

Drahos L, Vékey K. 1999a. Determination of the thermal energy and its distribution in peptides. J Am Soc Mass Spectrom 10:323–328.

Drahos L, Vékey K. 1999b. How closely related are the effective and the real temperature. J Mass Spectrom 34:79–84.

Drahos L, Vékey K. 2001. MassKinetics: A theoretical model of mass spectra incorporating physical processes, reaction kinetics and mathematical descriptions. J Mass Spectrom 36:237–263.

Drahos L, Heeren RMA, Collette C, De Pauw E, Vékey K. 1999. Thermal energy distributions observed in electrospray ionization. J Mass Spectrom 34:1373–1379.

Dreisewerd K. 2003. The desorption process in MALDI. Chem Rev 103:395–425.

Dunbar RC. 2004. BIRD (blackbody infrared radiative dissociation): Evolution, principles, and applications. Mass Spectrom Rev 23:127–158.

Dunbar RC, McMahon TB. 1998. Activation of unimolecular reactions by ambient blackbody radiation. Science 279:194–197.

Dunbar RC, Zaniewski RC. 1992. Infrared multiphoton dissociation of styrene ions by low-power continuous $CO_2$ laser irradiation. J Chem Phys 96:5069–5075.

Enke CG. 1997. A predictive model for matrix and analyte effects in electrospray ionization of singly-charged ionic analytes. Anal Chem 69: 4885–4893.

Ervin KM. 2000. Microcanonical analysis of the kinetic method. The meaning of the ''effective temperature.'' Int J Mass Spectrom 195(196): 271–284.

Forst W. 1973. The theory of unimolecular reactions. New York: Londres.

Gabelica V, De Pauw E, Karas M. 2004. Influence of the capillary temperature and the source pressure on the internal energy distribution of electrosprayed ions. Int J Mass Spectrom 231:189–195.

Gabelica V, De Pauw E. 2002. Comparison of the collision-induced dissociation of duplex DNA at different collision regimes: Evidence for a multistep dissociation mechanism. J Am Soc Mass Spectrom 13:91–98.

Gabelica V, Rosu F, Houssier C, De Pauw E. 2000. Gas phase thermal denaturation of an oligonucleotide duplex and its complexes with minor groove binders. Rapid Commun Mass Spectrom 14:464–467.

Gabelica V, Schulz E, Karas M. Internal energy build-up in matrix-assisted laser desorption/ionization. J Mass Spectrom (in press).

Gamero-Castaño M, Fernandez de la Mora J. 2000a. Kinetics of small ion evaporation from the charge and mass distribution of multiply charged clusters in electrosprays. J Mass Spectrom 35:790–803.

Gamero-Castaño M, Fernandez de la Mora J. 2000b. Mechanisms of electrospray ionization of singly and multiply charged salt clusters. Anal Chim Acta 406:67–91.

Garcia B, Ramirez J, Wong S, Lebrilla CB. 2001. Thermal dissociation of protonated cyclodextrin-amino acid complexes in the gas phase. Int J Mass Spectrom 210/211:215–222.

Gaskell SJ. 1997. Electrospray: Principles and practice. J Mass Spectrom 32: 677–688.

Gilbert RG, Smith SC. 1990. Theory of unimolecular and recombination reactions. Oxford.

Glückmann M, Karas M. 1999. The initial velocity and its dependence on matrix, analyte and preparation method in UV-MALDI. J Mass Spectrom 34:467–477.

Goeringer DE, McLuckey SA. 1996a. Evolution of ion internal energy during collisional excitation in the Paul ion trap: A stochastic approach. J Chem Phys 104:2214–2221.

Goeringer DE, McLuckey SA. 1996b. Kinetics of collision induced dissociation in the Paul trap: A first order model. Rapid Commun Mass Spectrom 10:328–334.

Gomez A, Tang K. 1994. Charge and fission of droplets in electrostatic sprays. Phys Fluids 6:404–414.

Greisch J-F, Gabelica V, Remacle F, De Pauw E. 2003. Thermometer ions for matrix-enhanced laser desorption/ionization internal energy calibration. Rapid Commun Mass Spectrom 17:1847–1854.

Griffin LL, McAdoo DJ. 1993. The effect of ion size on rate of dissociation: RRKM calculations on model large polypeptide ions. J Am Soc Mass Spectrom 4:11–15.

Griffiths WJ, Brown A, Reimendal R, Yang Y, Zhang J, Sjövall J. 1996. A comparison of fast-atom bombardment and electrospray as methods of ionization in the study of sulphated- and sulphonated-lipids by tandem mass spectrometry. Rapid Commun Mass Spectrom 10:1169–1174.

Harrison AG. 1999a. Energy-resolved mass spectrometry: Comparison of quadrupole cell and cone-voltage collision-induced dissociation. Rapid Commun Mass Spectrom 13:1663–1670.

Harrison AG. 1999b. Fragmentation reaction of alkylphenylammonium ions. J Mass Spectrom 34:1253–1273.

Hase WL. 1998. Some recent advances and remaining questions regarding unimolecular rate theory. Acc Chem Res 31:659–665.

Hayes JM, Small GJ. 1983. Supersonic jets, rotational cooling, and analytical chamistry. Anal Chem 55:565A–574A.

He F, Ramirez J, Garcia BA, Lebrilla CB. 1999. Differentially heated capillary for thermal dissociation of noncovalently bound complexes produced by electrospray ionization. Int J Mass Spectrom 182(183): 261–273.

Hirabayashi A, Sakairi M, Koizumi H. 1994. Sonic spray ionization method for atmospheric pressure ionization mass spectrometry. Anal Chem 66:4557–4559.

Hirabayashi A, Sakairi M, Koizumi H. 1995. Sonic spray mass spectrometry. Anal Chem 67:2878–2882.

Hirabayashi Y, Hirabayashi A, Takada Y, Sakairi M, Koizumi H. 1998. A sonic spray interface for the mass analysis of highly charged ions from protein solutions at high flow rates. Anal Chem 70:1882–1884.

Hiraoka K, Matsushita F, Hukasawa H. 1997. Enhancement of ion evaporation by the $CO_2$ laser irradiation on the electrospray and ionspray. Int J Mass Spectrom Ion Proc 162:35–44.

Hiraoka K, Saito S, Katsuragawa J, Kudaka I. 1998. A new liquid chromatography/mass spectrometry interface: Laser spray. Rapid Commun Mass Spectrom 12:1170–1174.

Hough JM, Haney CA, Voyksner RD, Bereman RD. 2000. Evaluation of electrospray transport CID for the generation of searchable libraries. Anal Chem 72:2265–2270.

Hoxha A, Collette C, De Pauw E, Leyh B. 2001. Mechanism of collisional heating in electrospray mass spectrometry: Ion trajectory calculations. J Phys Chem A 105:7326–7333.

Hunt SM, Sheil MM, Belov M, Derrick PJ. 1998. Probing the effect of cone potential in the electrospray ion source: Consequence for the determination of molecular weight distributions of synthetic polymers. Anal Chem 70:1812–1822.

Hunter CL, Mauk AG, Douglas DJ. 2000. Dissociation of heme from myoglobin and cytochrome b5: Comparison of behavior in solution and in the gas phase. Biochemistry 36:1018–1025.

Iavarone AT, Williams ER. 2003. Mechanism of charging and supercharging molecules in electrospray ionization. J Am Chem Soc 125:2319–2327.

Ikonomou MG, Blades AT, Kebarle P. 1991. Electrospray-IonSpray: A comparison of mechanism and performance. Anal Chem 63:1989–1998.

Iribarne JV, Dziedzic PJ, Thomson BA. 1983. Atmospheric pressure ion evaporation-mass spectrometry. Int J Mass Spectrom Ion Phys 50:331–347.

Iribarne JV, Thomson BA. 1976. On the evaporation of small ions from charged droplets. J Chem Phys 64:2287–2294.

Juraschek R, Dülcks T, Karas M. 1999. Nanoelectrospray—More than just a minimized-flow electrospray ionization source. J Am Soc Mass Spectrom 10:300–308.

Karas M, Hillenkamp F. 1988. Laser desorption ionization of proteins with molecular masses exceeding 10000 Daltons. Anal Chem 60:2299–2301.

Karas M, Krüger R. 2003. Ion formation in MALDI: The cluster ionization mechanism. Chem Rev 103:427–439.

Karas M, Bachmann D, Bahr U, Hillenkamp F. 1987. Matrix-assisted ultraviolet laser desorption of non-volatile compounds. Int J Mass Spectrom Ion Proc 78:53–68.

Katritzky AR, Watson CH, Dega-Szafran Z, Eyler J. 1990. Collisionally activated dissociation of *N*-alkylpyridinium cations to pyridine and alkyl cations in gas phase. J Am Chem Soc 112:2471–2478.

Kaufmann R, Kirsch D, Spengler B. 1994. Sequencing of peptides in a TOF mass spectrometer: Investigation of postsource decay following MALDI. Int J Mass Spectrom Ion Proc 131:355–385.

Kebarle P. 2000. A brief overview of the present status of the mechanisms involved in electrospray mass spectrometry. J Mass Spectrom 35:804–817.

Kebarle P, Peschke M. 2000. On the mechanisms by which the charged droplets produced by electrospray lead to gas phase ions. Anal Chim Acta 406:11–35.

Kebarle P, Tang L. 1993. From ions in solution to ions in the gas phase. Anal Chem 65:972A–986A.

Kenttämaa HI, Cooks RG. 1985. Internal energy distributions acquired through collisional activation at low and high energies. Int J Mass Spectrom Ion Proc 64:79–83.

Kilby GW, Sheil MM. 1993. Effect of electrospray ionization conditions on low energy tandem mass spectra of peptides. Org Mass Spectrom 28: 1417–1423.

Kleinekofort W, Avdiev J, Brutschy B. 1996. A new method of laser desorption mass spectrometry for the study of biological macromolecules. Int J Mass Spectrom Ion Proc 152:135–142.

Kleinekofort W, Pfenninger A, Plomer T, Griesinger C, Brutschy B. 1996. Observation of noncovalent complexes using laser-induced liquid beam ionization/desorption. Int J Mass Spectrom Ion Proc 156:195–202.

Kleinekofort W, Schweitzer M, Engels JW, Brutschy B. 1997. Analysis of double-stranded oligonucleotides by laser-induced liquid beam mass spectrometry. Int J Mass Spectrom Ion Proc 163:1L–4L.

Knochenmuss R, Zenobi R. 2003. MALDI ionization: The role of in-plume processes. Chem Rev 103:441–452.

Kudaka I, Kojima T, Saito S, Hiraoka K. 2000. A comparative study of laser spray and electrospray. Rapid Commun Mass Spectrom 14:1558–1562.

Laprévote O, Ducrot P, Thal C, Serani L, Das BC. 1996. Stereochemistry of electrosprayed ions. Indoloquinolizidine derivatives. J Mass Spectrom 31:1149–1155.

Laskin J, Futrell JH. 2003. Entropy is the major driving force for fragmentation of proteins and protein–ligand complexes in the gas phase. J Phys Chem A 107:5836–5839.

Lifshitz C. 1982. Time-resolved appearance energies, breakdown graphs, and mass spectra: The elusive ''kinetic shift.'' Mass Spectrom Rev 1:309–348.

Light-Wahl KJ, Schwartz BL, Smith RD. 1994. Observation of non-covalent quaternary associations of proteins by electrospray ionization mass spectrometry. J Am Chem Soc 116:5271–5278.

Lips AGAM, Lameijer W, Fokkens RH, Nibbering NMM. 2001. Methodology for the developquent of a drug library based upon collision-induced fragmentation for the identification of toxicologically relevant drugs in plasma samples. J Chromatogr B 759:191–207.

Loo JA, Udseth HR, Smith RD. 1988. Collisional effects on the charge distribution of ions from large molecules, formed by electrospray ionization mass spectrometry. Rapid Commun Mass Spectrom 2:207–212.

Lorquet JC. 2000. Landmarks in the theory of mass spectra. Int J Mass Spectrom 200:43–56.

Luo G, Marginean I, Vertes A. 2002. Internal energy of ions generated by matrix-assisted laser desorption/ionization. Anal Chem 74:6185–6190.

Marquet P, Venisse N, Lacassie E, Lachâtre G. 2000. In-source CID mass spectral libraries for ''general unknown'' screening of drugs and toxicants. Analusis 28:925–934.

Mayer PM, Baer T. 1996. A photoionizaation study of vibrational cooling in molecular beams. Int J Mass Spectrom Ion Proc 156:133–139.

McLuckey SA. 1991. Principles of collisional activation in analytical mass spectrometry. J Am Soc Mass Spectrom 3:599–614.

Melnyk MC, Schey KL, Bartlett MG, Busch KL. 1998. Charge-remote fragmentation in dialkylaminosteryl dyes. J Mass Spectrom 33:850–857.

Meot-Ner (Mautner) M, Dongré A, Somogyi A, Wysocki VH. 1995. Thermal decomposition kinetics of protonated peptides and peptide dimers, and comparison with surface induced dissociation. Rapid Commun Mass Spectrom 9:829–836.

Mowry CD, Johnston MV. 1994. Internal energy of neutral molecules ejected by MALDI. J Phys Chem 98:1904–1909.

Penn SG, Cancilla MT, Green MK, Lebrilla CB. 1997a. Direct comparison of matrix-assisted laser desorption/ionization and electrospray ionisation in the analysis of gangliosides by Fourier transform mass spectrometry. Eur Mass Spectrom 3:67–79.

Penn SG, He F, Green MK, Lebrilla CB. 1997b. The use of heated capillary dissociation and collision-induced dissociation to determine the strength of non-covalent bonding interactions in gas-phase peptide-cyclodextrin complexes. J Am Soc Mass Spectrom 8:244–252.

Pertel R. 1975. Molecular beam sampling of dynamic systems. Int J Mass Spectrom Ion Phys 16:39–52.

Price WD, Williams ER. 1997. Activation of peptide ions by blackbody radiation: Factors that lead to dissociation kinetics in the rapid energy exchange limit. J Phys Chem A 101:8844–8852.

Ramanathan R, Prokai L. 1995. Electrospray ionization mass spectrometric study of encapsulation of amino acids by cyclodextrins. J Am Soc Mass Spectrom 6:866–871.

Raznikov VV, Kozlovsky VI, Dodonov AF, Raznikova MO. 1999. Heating of ions moving in a gas under the influence of a uniform and constant electric field. Rapid Commun Mass Spectrom 13:370–375.

Rockwood AL, Busman M, Udseth HR, Smith RD. 1991. Thermally induced dissociation of ions from electrospray mass spectrometry. Rapid Commun Mass Spectrom 5:582–585.

Rogniaux H, Van Dorsselaer A, Barth P, Biellmann JF, Brabanton J, van Zandt M, Chevrier B, Howard E, Mitschler A, Potier N, Urzhumtseva L, Moras D, Podjarny A. 1999. Binding of aldose reductase inhibitors: Correlation of crystallographic and mass spectrometric studies. J Am Soc Mass Spectrom 10:635–647.

Rostom AA, Tame JRH, Ladbury JE, Robinson CV. 2000. Specificity and interactions of the protein OppA: Partitioning solvent binding effects using mass spectrometry. J Mol Biol 296:269–279.

Sakamoto S, Imamoto T, Yamaguchi K. 2001. Constitution of Grignard reagents RMgCl in tetrahydrofuran. Org Lett 3:1793–1795.

Sakamoto S, Yamaguchi K. 2003. Hyperstranded DNA architectures observed by cold-spray ionization mass spectrometry. Angew Chem Int Ed 42:905–908.

Sakamoto S, Fujita M, Kim K, Yamaguchi K. 2000. Characterization of self-assmebling nano-sized structures by means of coldspray ionization mass spectrometry. Tetrahedron 56:955–964.

Sakamoto S, Nakatani K, Saito I, Yamaguchi K. 2003. Formation and destruction of the guanine quartet in solution observed by cold-spray ionization mass spectrometry. Chem Commun 788–789.

Schmelzeisen-Redeker G, Bütfering L, Röllgen FW. 1989. Desolvation of ions and molecules in thermospray mass spectrometry. Int J Mass Spectrom Ion Proc 90:139–150.

Schmidt A, Bahr U, Karas M. 2001. Influence of pressure in the first pumping stage on analyte desolvation and fragmenation in nano-ESI MS. Anal Chem 73:6040–6046.

Schneider BB, Douglas DJ, Chen DDY. 2001. Ion fragmentation in an electrospray ionization mass spectrometer interface with different gases. Rapid Commun Mass Spectrom 15:249–257.

Schneider BB, Chen DDY. 2000. Collision-induced dissociation of ions within the orifice-skimmer region of an electrospray mass spectrometer. Anal Chem 72:791–799.

Seto C, Grossert JS, Waddell DS, Curtis JM, Boyd RK. 2001. Effects of ionization mode on charge-site-remote and related fragmentation reactions of long-chain quaternary ammonium ions. J Am Soc Mass Spectrom 12:571–579.

Shulka AK, Futrell JH. 1993. Collisional activation and dissociation of polyatomic ions. Mass Spectrom Rev 12:211–255.

Shulka AK, Futrell JH. 2000. Tandem mass spectrometry: Dissociation of ions by collisional activation. J Mass Spectrom 35:1069–1090.

Smith RD, Barinaga CJ. 1990. Internal energy effects in the collision-induced dissociation of large biopolymer molecular ions produced by electrospray ionization tandem mass spectrometry of cytochrome *c*. Rapid Commun Mass Spectrom 4:54–57.

Sobott F, Wattenberg A, Kleinekofort W, Pfenninger A, Brutschy B. 1998. Laser desorption mass spectrometry on thin liquid jets. Fresenius J Anal Chem 360:745–749.

Spengler B. 1997. Postsource decay analysis in MALDI- MS of biomolecules. J Mass Spectrom 32:1019–1036.

Spengler B, Kirsch D, Kaufmann R. 1992. Fundamental aspects of postsource decay in MALDI mass spectrometry. J Phys Chem 96:9678–9684.

Steinfeld JI, Francisco JS, Hase WL. 1999. Chemical kinetics and dynamics. New Jersey: Prentice Hall.

Takats Z, Drahos L, Schlosser G, Vékey K. 2002. Feasibility of formation of hot ions in electrospray. Anal Chem 74:6427–6429.

Takats Z, Nanita SC, Cooks RG, Schlosser G, Vékey K. 2003. Amino acid clusters formed by sonic spray ionization. Anal Chem 75:1514–1523.

Takayama M, Fukai T, Nomura T, Nojima K. 1990. Further study of the matrix effect on the extent of fragmentation in molecular ions M+. produced under fast atom bombardment (FAB) conditions. Int J Mass Spectrom Ion Proc 96:169–179.

Thierolf M, Bahr U, Karas M. 1997. Which matrix properties determine if MALDI ions survive or die (fragment) ? Proceedings of the 45th ASMS Conference on Mass Spectrometry and Allied Topics. 856.

Thomson BA, Iribarne JV. 1979. Field induced ion evaporation from liquid surfaces at atmospheric pressure. J Chem Phys 71:4451–4463.

van Dongen WD, van Wijk JIT, Green BN, Heerma W, Haverkamp J. 1999. Comparison between collision induced dissociation of electrosprayed protonated peptides in the up-front source region and in a low-energy collision cell. Rapid Commun Mass Spectrom 13:1712–1716.

Vertes A, Irinyi G, Gijbels R. 1993. Hydrodynamic model of MALDI mass spectrometry. Anal Chem 65:2389–2393.

Voyksner RD, Pack T. 1991. Investigation of collisional-activation decomposition process and spectra in the transport region of an electrospray single quadrupole mass spectrometer. Rapid Commun Mass Spectrom 5:263–268.

Vékey K. 1996. Internal energy effects in mass spectrometry. J Mass Spectrom 31:445–463.

Wang G, Cole RB. 2000. Charged residue versus ion evaporation for formation of alkali metal halide clusters in ESI. Anal Chim Acta 406: 53–65.

Wattenberg A, Sobott F, Brutschy B. 2000. Detection of intact hemoglobin from aqueous solution with laser desorption mass spectrometry. Rapid Commun Mass Spectrom 14:859–861.

Wattenberg A, Sobott F, Barth H-D, Brutschy B. 1999. Laser desorption mass spectrometry on liquid beams. Eur Mass Spectrom 5:71–76.

Wattenberg A, Sobott F, Barth H-D, Brutschy B. 2000. Studying noncovanent protein complexes in aqueous solution with laser desorption mass spectrometry. Int J Mass Spectrom 203:49–57.

Weinmann W, Wiedemann A, Eppinger B, Renz M, Svoboda M. 1999. Screening for drugs in serum by electrospray ionization/collision-induced dissociation and library searching. J Am Soc Mass Spectrom 10:1028–1037.

Weinmann W, Stoertzel M, Vogt S, Svoboda M, Schreiber A. 2001a. Tuning compounds for electrospray ionization/in-source CID and mass spectra library searching. J Mass Spectrom 36:1013–1023.

Weinmann W, Stoertzel M, Vogt S, Wendt J. 2001b. Tune compounds for electrospray ionization/in-source CID with mass spectral library searching. J Chromatogr A 926:199–209.

Whitehouse M, Dreyer RN, Yamashita M, Fenn JB. 1985. Electrospray interface for liquid chromatographs and mass spectrometers. Anal Chem 57:675–679.

Wilm M, Mann M. 1996. Analytical properties of the nanoelectrospray ion source. Anal Chem 68:1–8.

Wysocki VH, Kenttämaa HI, Cooks RG. 1987. Internal energy distributions of isolated ions after activation by various methods. Int J Mass Spectrom Ion Proc 75:181–208.

Yamaguchi K. 2003. Cold-spray ionization mass spectrometry: Principle and applications. J Mass Spectrom 38:473–490.

Yamashita M, Fenn JB. 1984. Electrospray ion source. Another variation on the free-jet theme. J Phys Chem 88:4451–4459.

Zenobi R, Knochenmuss R. 1998. Ion formation in MALDI mass spectrometry. Mass Spectrom Rev 17:337–366.

---

**Valérie Gabelica** conducted her Ph.D. thesis on the study of non-covalent complexes by electrospray mass spectrometery under the direction of Prof. De Pauw (University of Liège) from 1998 to 2002. She spent one year (Oct. 2002-Sept. 2003) in the group of Prof. Karas (Universität Frankfurt, Germany), sponsored by the Alexander von Humboldt Foundation, working on internal energy aspects of ESI, MALDI and quadrupole ion trap CID. She is now back in the Mass Spectrometry Laboratory at the University of Liège as an FNRS post-doctoral research fellow, and is working on fundamentals and applications of MS to the study of biomolecular interactions.

**Edwin De Pauw** conducted his Ph.D. thesis on the photochemistry of charge transfer complexes. His annex thesis was focused on the application of Secondary Ion Mass Spectrometery to inorganic and organic molecular solids. After his thesis (1981), he spent one year in the group of F.W. Roellgen, thanks to a postdoctoral fellowship from the A. von Humboldt Foundation. Back in Liège University, he started working on Liquid SIMS in the Physical Chemistry Department where he obtained a permanent position in 1986. He spent five years as Research Scientist at the European Commission; first at Joint Research Center (Environment Institute, 1987–1990), second at the Patent Office of the Commission (DG13, Luxembourg, 1990–1991). He came back to Liege University in 1991 as associate Professor and initiated the Mass Spectrometry Laboratory. He is the confounder of the Center for the Analysis of Residues at Trace Levels (CART, 1999) and its acting Director. He is a member of the steering committee of the Genoproteomic Center (GIGA), responsible for the proteomic unit. He became a Full Professor in January 2003.